Investigation of Novel Solutions to Integrate Organic Rankine Cycle Power Systems on Ships

BSc.Eng. Project

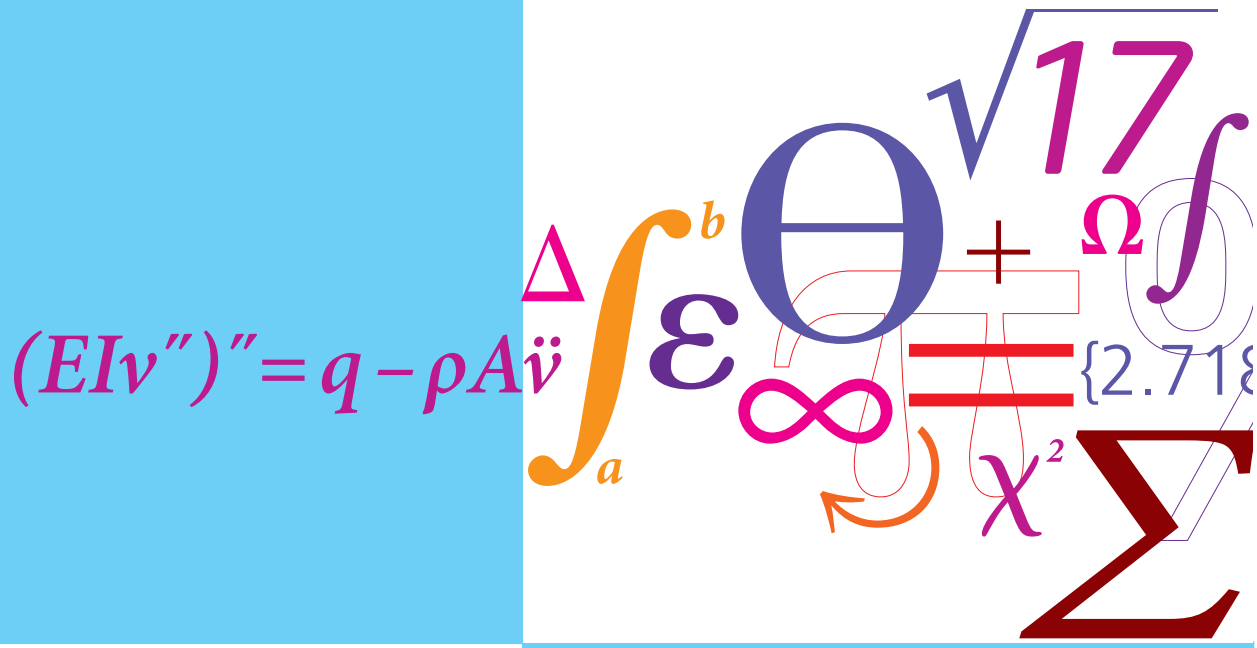

Sergio Quetglas Blancher
June 2018

DTU Mechanical Engineering
Department of Mechanical Engineering

DTU Mechanical Engineering
Section of Thermal Energy
Technical University of Denmark

Nils Koppels Allé, Bld. 403
DK-2800 Kgs. Lyngby
Denmark
Phone (+45) 4525 4131
Fax (+45) 4588 4325

www.mek.dtu.dk

Contents

1 Abstract **2**

2 Nomenclature **2**

3 Introduction **3**

4 ORC technology **3**

5 Description of the System **4**
5.1 ORC Boiler 5
5.1.1 Pinch Point 7
5.2 Condenser 8
5.3 Pump 8
5.4 Expander 8
5.4.1 Multi-Vane Expander 9
5.4.2 Screw Expander 9
5.4.3 Scroll Expander 10
5.4.4 Piston expander 10
5.5 Working Fluid selection 11

6 Modelling of the ORC system **12**
6.1 Configuration I. 13
6.2 Configuration II. 15
6.3 Configuration III. 16

7 Results and discussion **17**
7.1 Results for Configuration I. 17
7.2 Results for Configuration II. 19
7.3 Results for Configuration III. 21
7.4 Influence of the Steam Requirement between configurations compared to the maximum power assumption. 23
7.5 Discussion. 25

8 Conclusion **27**

9 Acknowledgements **27**

1 Abstract

Emissions in engines is one of the main concern in terms of pollutant investigation nowadays as well as to reduce fuel consumption. Two-stroke diesel engines is a frequent propulsion system used in ships. They are characterized by a high efficiency due to their high compression ratio, however, half of the energy generated by the fuel is dissipated as heat. To harvest this heat loss, the Organic Rankine Cycle, ORC, fits the requirement as it is characterized by its ability to harvest heat from low-temperature sources.

This project define three different configurations using five different working fluids where the ORC is used as a heat recovery system in a vessel. The steam generation by means of using a HRSG and how it affects to the system will be studied too. A technological overview of the ORC and their different components will be described briefly in the first part of the project. The results showed that ORC system can generate up to 2 MW for some configurations. Moreover, the configuration were modelled to keep a pinch point of 15 K to increase the efficiency of the ORC unit.

2 Nomenclature

HRSG	*Heat Recovery Steam Generator*	c_p	*Specific Heat*
RC	*Rankine Cycle*	T_{inl}	*Inlet Temperature*
SRC	*Steam Rankine Cycle*	T_{out}	*Outlet Temperature*
ORC	*Organic Rankine Cycle*	$T_{inl,expand}$	*Inlet temperature of the turbine*
HEX	*Heat Exchanger*	$T_{out,boil}$	*Outlet temperature of the ORC boiler*
UA	*Heat transfer coefficient times the Area*	T_{evap}	*Temperature of the Evaporator*
NPP	*Net Power Production*	dT_{sup}	*Degree of Superheating*
HSR	*High Steam Requirement*	$\eta_{p,t}$	*Efficiency of the pump or turbine*
LSR	*Low Steam Requirement*	$\dot{m}_{orc}$	*Organic fluid massflow*
EG	*Exhaust Gases*	$\dot{W}_{pump}$	*Power absorbed by the pump*
$\dot{Q}$	*Heat transferred*	$\dot{W}_{turb}$	*Power generated by*
$\dot{m}_{ex}$	*Exhaust Gas massflow*	$\dot{W}_{net}$	*Net power*

3 Introduction

International maritime shipping represents 2.7 % of global greenhouse emissions. Greenhouse emissions as well as pollutants is one of the main concerns nowadays [1]. Most of the ship fleet is powered by internal combustion (IC) engines [2]. Diesel engines are one of the most common propulsion system in ships. Diesel engines for marine applications have the highest efficiency due to the higher compression ratio that they work with [3]. Nevertheless, around half of the power input is lost through exhaust gases, cooling water (high and low temperature) and a very small part in heat radiation as seen in Figure 1

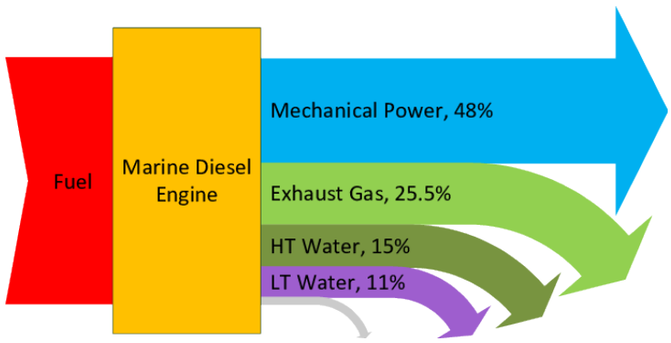

Figure 1: Energy distribution in a marine engine [3].

This energy loss due to refrigeration or heat loss makes possible to install diverse equipment to profit the heat release to, for example, produce service steam that will be used in different parts of the ship e.g. air conditioning, boilers, laundry, etc. To produce the steam harvesting the heat lost a Heat Recovery Steam Generator [HRSG] is used. Normally, the type of Heat exchanger, HEx, used for steam generation is with finned tubes, where the steam will flow through the tubes and the exhaust gases will pass through the shell [2]. As can be seen in the Figure 1, three main ways of using the heat released can be applied. New ways of implementing other systems to produce energy into the ship are being studied nowadays to harvest the remaining heat used in the HRSG as well. Using steam through the Rankine Cycle, SRC, is a well-known mean of power production, however, for lower temperatures its efficiency drops. Nevertheless, Rankine cycle using an organic fluid, ORC, becomes a feasible option to produce energy when low temperature sources are used [4].

4 ORC technology

In this section, a brief review of the organic Rankine cycle, ORC, technology will be discussed. The Rankine cycle, RC, is a well-known process that is used for power production even though it can be also used in the refrigeration field using the reverse configuration. It normally works at temperatures oscillating between 250-600 ^{o}C what makes its Carnot efficiency impractical for low application temperatures [5]. Still, by using an organic fluid, it is possible to harvest the heat from a low-temperature heat source.

In the direct Rankine cycle a fluid is compressed in the first phase using commonly a pump that will increase the pressure in the fluid that is in liquid state i.e water in liquid state for the steam rankine cycle, SRC. After the compression phase the fluid is heated through a heat exchanger, this component can be divided in three phases, preheating, evaporator and superheater. In this system, the heat source will be the exhaust gases of the engine or the jacket water that has been used to cool the engine. After the heating section, the fluid will go through a expander i.e. a turbine. It is the gradient of pressure and temperature what the system benefits to produce electricity during the expansion phase. Besides, depending on the temperature difference there will be a different pressure drop for each fluid. The different configurations of expanders will be examined in the expander section below. In the last part of the fluid, it is cooled down by using a condenser. A condenser is basically a heat exchanger that, using a cold source, cools the fluid and therefore, turn it into the liquid phase to be compressed again.

The ORC owes its name to the working fluid inside the closed system. This organic fluid is characterised by a high molecular mass fluid and a lower boiling point, this, compared to the steam-RC makes it possible to use in low temperature applications. In Figure 2, different temperatures

range are displayed, as can be seen, the temperature boundaries go from 70-100 °C to 200-250 °C or above. For temperatures below the low value, the costs of the system makes it not economically feasible [6]. In any case, the development of this technology is nowadays growing vastly because of the research of new solutions and configurations for the system specially in the field of renewable energies [7] because of its potential and flexibility to adapt to many scenarios e.g. different heat sources like exhaust gases, geothermal sources. Figure 2 shows the different application fields of an ORC depending on the temperature of the heat source and the power output [6].

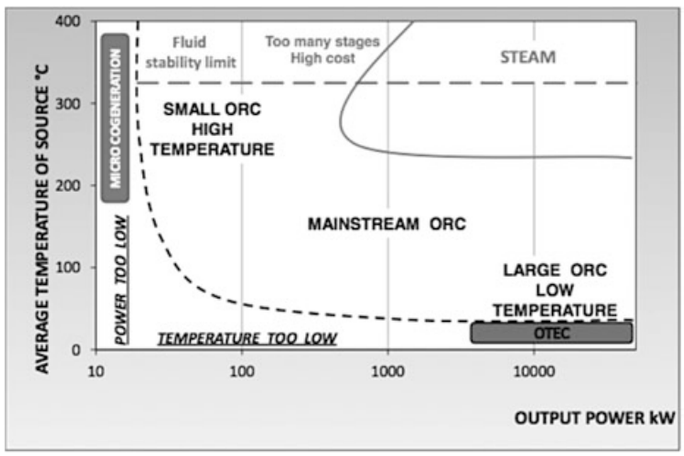

Figure 2: Application Fields of ORC depending on temperature of heat source [6].

5 Description of the System

The characterization of the ORC system will be discussed. The values used for the reference case for steam production and the inlet temperature as well as the mass flow of the exhaust gases come from the 8S70ME-GI engine with low pressure SCR tuning, that has a power output of 23 MW. Two different steam requirements will be studied. 1730 and 865 kg/h of steam demand will be used as reference case. For this system, two main heat sources can be used in many ways. Exhaust gases and Jacket water cooling are proper heat sources that can be used in the ORC unit, however, in this study, only the utilization of exhaust gases will be carried out.

Jacket water cooling is also an available heat source for the system. It will be used directly for the ORC boiler and the water will be used as heat source in this case. The presence of sulphur in some fuels used for marine application may result in corrosion of the tubes used in the heat exchanger of the ORC Boiler, whereas when using water as a heat source, there is no sulphur substances through the tubes, avoiding fast corrosion of components [2]. Regarding the thermal properties of the jacket water, it will have lower inlet temperature but its specific heat is 4 times higher compared to the exhaust gases value [8]. However, the utilization of jacket water cooling as a heat source will not be studied for this bachelor thesis so, further investigation could be done in this field. There is also a second heat exchanger that will be working as a condenser right after the turbine, it will be using the sea water as a cold source. [9]. Figure 3 shows the diagram of the ORC without an intermediate loop between the heat source and the ORC boiler.

For this project, three different configurations will be studied. Starting from a simple layout, where the exhaust gases go firstly through a heat recovery steam generator to produce the required amount of demanded steam and then, the remaining heat of the exhaust gases will be used to vaporize the organic fluid that will flow through the ORC boiler. Other option for the exhaust gases will be the split of the total mass flow, sending one part to the HRSG and other part to the ORC boiler directly, for this configuration, different massflow distribution will be carried out to see the performance of the ORC system. In the last configuration, the exhaust gases will flow through the ORC system and then will go through the HRSG.

Regarding the ORC unit, Figure 3, the organic fluid is compressed first in the pump until reaching a designed value. The pump also has to regulate the amount of massflow through the system as it will vary depend on the steam requirement or the engine load. Once the fuel is compressed, the fluid flow through the ORC boiler. The ORC boiler can be divided in three phases, first a preheating part where the fluid is heated up until the evaporation temperature, then it flows through the boiler where all the fluid is evaporated and last, the fluid goes through a superheating phase where the temperature of the gas is increased. Afterwards, the organic fluid

goes through the expander where the power is generated by the expansion of the working fluid through an expander that will make an axis rotate and this will be connected to a generator. To close the cycle, the fluid is cooled down in the condenser using sea water as cold source.

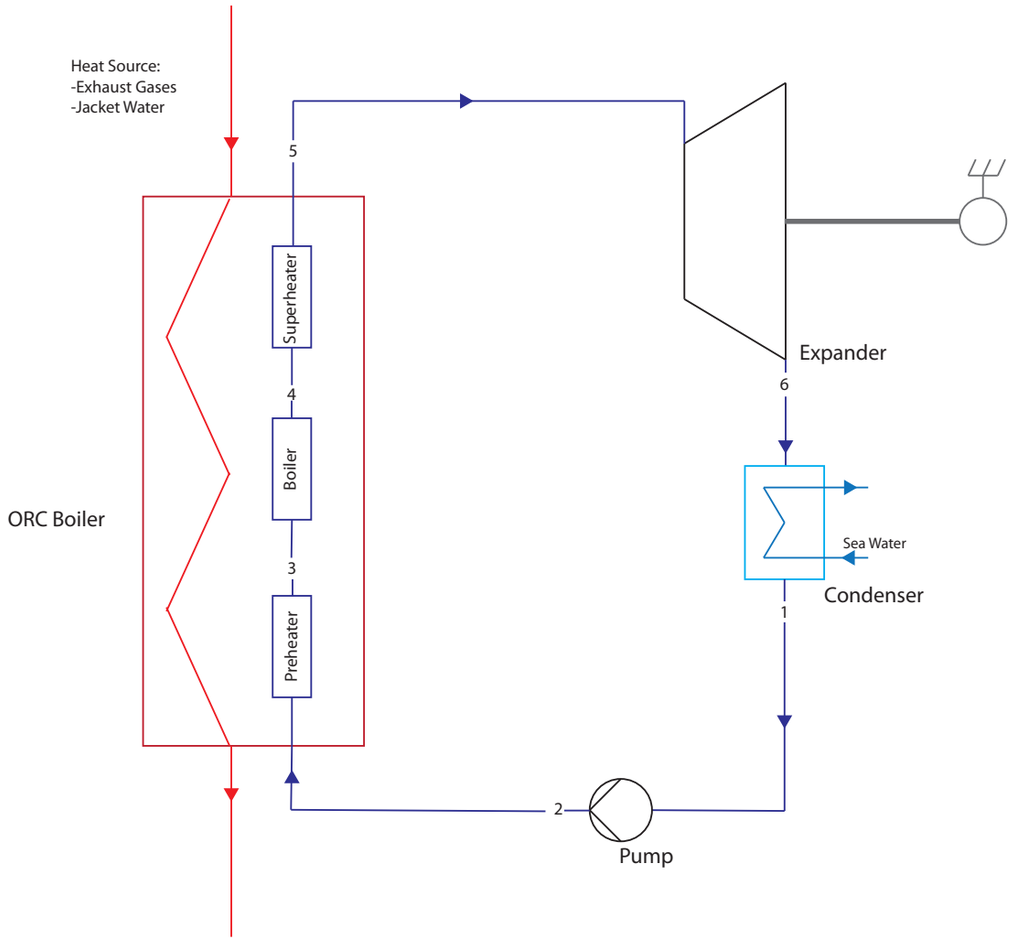

Figure 3: Diagram of ORC without intermediate loops.

Nevertheless, the control of the system has to be optimised in order to get the best performance of the system. It requires a great complexity to control the load of the pump as well as the speed of the turbine as it has to be changed constantly because the heat source is continually changing [10].

5.1 ORC Boiler

The set of heat exchangers in the ORC system can represent the 30 % of the total cost [4]. Besides, the space occupied by the equipment is another factor to keep in mind as in ships is an important aspect [2] due to the space is limited on board. This, makes its design and optimization inside the system one of the most important elements of the project, additionally, the total area of them can reach large values, so, it has to be studied carefully by the detailed observation of the pinch point [10]. Organic fluids are characterised by a smaller density difference between the vapour and liquid phase what allows the design of once-trough boilers avoiding re-circulation of flows Moreover, once-through boilers are characterised by the absence of drums [10]. Furthermore, the ORC working fluid flows through a continuous way, with no physical division between economizer, evaporator and superheater [11] providing a high adaptability to the required load of the expander. In the following figure 4 a one-through steam generator is shown.

Figure 4: Once-through steam generator used in Gorizia Combined cycle Power Plant [12].

The different types of heat exchanger will be analysed. Figure 5 shows two different types of HEx that can be utilised. Finned tube boilers for ORC units can be used. This type of heat exchangers ensure high-compactness due to its high *heat transfer area-to-volume* [2]. As well as the finned tube boilers, the fin-plate heat exchanger can be a good choice to use as a heat exchanger for the naval field as it is also characterised by a high *heat transfer area-to-volume* too. In addition, the weight of fin plate heat exchangers can be ten times lower compared to finned tube boilers, still, its cost and the maintenance required to keep the channels unblocked to avoid pressure drops through the boiler is a relevant drawback when using fin-plate heat exchangers [2]. Regarding the employment of plate heat exchangers can be used on small ships, where the flow rate is limited. Lastly, for the flow configuration in a heat exchanger, a counter-flow configuration will be the most suitable concerning the saving-investment ratio [13]. In the following picture, some type of heat exchangers are displayed.

Figure 5: Plate-finned HEX designed by Linde AG (left) and welded plates HEX designed by Danfoss (right) [14]-[15].

Regarding the heat source, there are many ways of configuring the ORC. Exhaust Gases, Lubricating oil from the engine, Jacket water cooling, Scavenge air and EGR [2] and[10] can be used as a heat source in the ORC system, however in this project only it will be studied the exhaust gases.

In relation to HEX architecture, it can be divided in three main parts: preheater or economizer, evaporator and superheater [16]. In the economizer, the fluid is in liquid phase and the main function of this part is to heat up the working fluid. Once the organic fluid reaches the evaporation temperature, the evaporation of the fluid begins. In this part, a phase change of the fluid occurs, meaning that the temperature of the process will keep constant temperature. In the end, when the fluid is fully evaporated, a superheating phase will occur. As well as in the preheater, the temperature raises following a linear relation [17]. In this project the degree of superheating will be optimised by using EES. The T-Q diagram of a single-pressure heat exchanger is showed in the following figure 6.

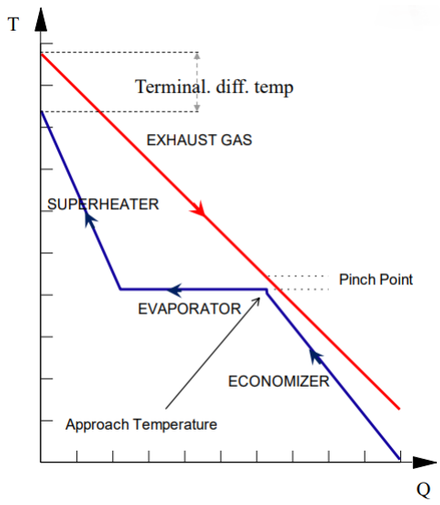

Figure 6: T-Q diagram for a single pressure HEX [16].

For the boiler configuration, two approaches can be taken into account. First, the heat can be transferred directly from heat source, i.e., exhaust gases or jacket water cooling. Direct heating attains higher outlet temperatures of the cold side from the HEX, increasing the efficiency of itself, according to Colonna et al [7]. On the other hand, the utilisation of an intermediate loop between the heat source and the organic fluid can help in terms of controlling the unit due to the variations of the heat source during its operations [2]. Furthermore, the installation of an intermediate loop using oil or other substance protects the working fluid as it degrades in the start-stop cycles. However, this equipment increases the complexity and the final price of the system, besides, supplementary pumping energy would be needed [7].

5.1.1 Pinch Point

The pinch point is one of the most important variables regarding design of HEX. In concern of the pinch point numeric value, there is a minimum temperature difference that has to be kept over it [4]. This temperature can be set in three different parts of the HEX, for this project the pinch point will be set in the part where the evaporation phase begins as well as the outlet of the gases, later on, the lowest value of ORC massflow will be used. The pinch point can be set between 5 and 20 K of difference depending on the heat source used. [2]. Furthermore, an optimum value from 15 to 20 K of pinch point for an internal combustion engine can increase the efficiency up to 7% of the system [18].
Regarding the efficiency and of the ORC, Wang et al. defined a coefficient called k that is a ratio between the pinch point of the evaporator and the condenser [19].

$$k = \frac{\Delta T_e}{\Delta T_c}$$

As it can be seen in the following figure 7, as it increases the value of k, meaning that the temperature difference in the evaporator is larger, the efficiency of the ORC system increases. According to J. Wang et al. the efficiency increases relentlessly with k because even when the net power production decreases because this reduction is less than the heat absorpted by the HEX [19], whereas for the net power output of the turbine, its behaviour depends on the type of working fluid used in the assembly .

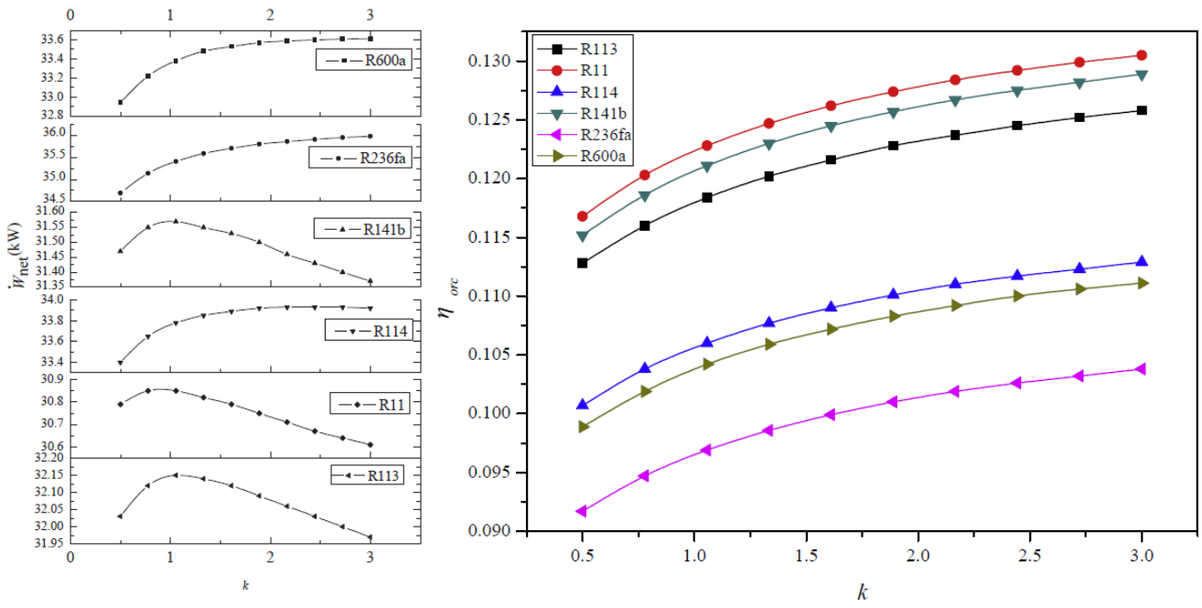

Figure 7: Influence of k on NPP (left) and Thermal efficiency depending on k (right) for different working fluids in an ORC [19].

5.2 Condenser

In this section, the condensation phase of the ORC fluid will be discussed. After the expansion in the turbine, most of the fluid still in steam phase, i.e., for some working fluids, as the inlet pressure of the turbine is increased, some droplets are found after the expansion phase. Therefore, in order to ensure that in the inlet of the pump all the organic fluid is in liquid phase, a condensation phase is required. To cool down the organic fluid, sea water will be used as cold source in the condenser. The seawater temperature will involve a minimum temperature of the organic fluid.

The condenser can represent a high cost in the installation, thus, in some cases the selection of an ORC including a regenerator could help to reduce the total size of the condenser making it more compact as both of them will be in the same insulated housing [7].

5.3 Pump

ORC pumps are one of the basic components in the ORC system, e.g, heat exchanger, turbine, condenser and pump. Pumps are characterized by their variability in terms on efficiency depending on the operating conditions. For this reason, controllability will be one of the key factors in pumps [10]. Besides, the pumping power can represent up to 10 % of the power output, justifying its importance in terms of optimization [2].

The utilization of positive displacement and centrifugal pumps will be discussed. Positive displacement or volumetric pumps are characterized for having efficiencies around 40 %. Volumetric pumps are restricted to lower NPP output, around 50 kW, for this reason, this type of pumps would not be possible to use in this configuration as the power outputs are relatively high due to the heat source used. On the other hand, centrifugal pumps have not a volumetric limitation, meaning that they can be used for high power output. Centrifugal pumps have higher efficiencies compared to positive displacement pumps, up to 60 %, also, their volumetric rate depends on the rotational speed as well as for the pressure ratio [2].

Pumps in ORC systems will control the fluid mass flow rate [10]. Habitually, to control the operative point of the pump, the rotational speed is varied. However, the massflow variation when the system is operating at part-load, i.e., off-design conditions, also relies on the part-load conditions of the other components such as heat exchanger and expander [2].

5.4 Expander

Mostly ORC working fluids have an expansion process completely dry, this avoids blade erosion issues in turbines and inherent expansion inefficiency due to condensation. For ORC technology there are many types that can be used. Deciding an optimum expander for the ORC system is crucial and it will depend on the heat source, the conditions on the system and lastly, the total

size of the system e.g. power output [4].

They can be classified in dynamic and volumetric expanders [7].Dynamic expanders are normally turbines. In turbines, the fluid is past through the turbine blades at high temperature and pressure, making the blades rotate while the gas is expanding. This expansion work is harvested by connecting the shaft of the turbine to an electrical generator. For the shaft configuration, two ways can be axial or centrifugal. The axial configuration is more common when a high net power and mass flow is required, besides it is characterised for a higher efficiency[5]. Nevertheless, for a small power output application, the cost and manufacture is rather costly and it increase with the number of stages of the turbine in axial configuration besides its high rotatory speed that has to be decreased through a gear to work with an electric generator [5]. Centrifugal turbines can be used in low mass flow cases [2].

The volumetric expander have a determined volume ratio. They can be classified as rotary vane expander, piston expander, screw expander and scroll expander. They are defined for having lower mass flow rates compared to turbines. In volumetric expander, the expansion is produced by an increase of the area inside the body. Volumetric expanders are suitable for low NPP ORC for waste recovery units according to many studies [20]

5.4.1 Multi-Vane Expander

Multi-Vane expander is a volumetric expander. They have a simple structure, besides, their torque as well as the volumetric efficiency is relatively high as well as the temperature and pressure [20]. They are characterised by a rotor that turns eccentrically, while the vanes keep contact with the walls of the expander during all the rotation. One of its best characteristic is the consistent efficiency in different operating conditions. They normally work at low speed, what allows to connect directly to the generator or using simple gearboxes [5]. In the following figure 8, the working principle as well as the parts of a multi-vane expander are showed.

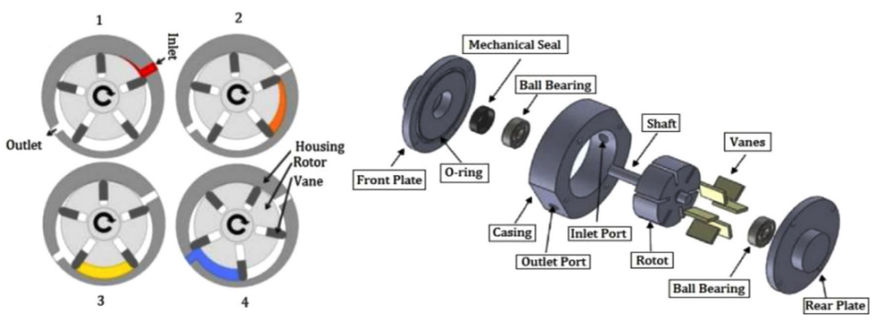

Figure 8: Working principle and components of vane expander [20]

5.4.2 Screw Expander

The screw expander is formed by two helical rotors. They rotate against each other as the fluid expands along the screws. This expansion work is connected directly to a single shaft [5] .
They can work from 2 to 10 of pressure ratio, and they cover a vast range of NPP (from 1.5 kW to 1MW. However, for NPP lower than 10 kW it is not recommended to use them as the cost of the expander increases due to specific requirements in tolerance due to leakage. One disadvantage is that they have a rather high rotation speed so they demand a gearbox to adapt the rotational speed [20]. As all volumetric expanders, the seal is a rather important part of the design to reduce the internal leakage. To avoid leakages during the expansion process, oil can be injected. Injecting oil is more simple regarding mechanical design, apart of having a high efficiency. Also, oil injection is cheaper than oil-free lubrication [5]. The figure 9 displays an scroll expander and its working principle.

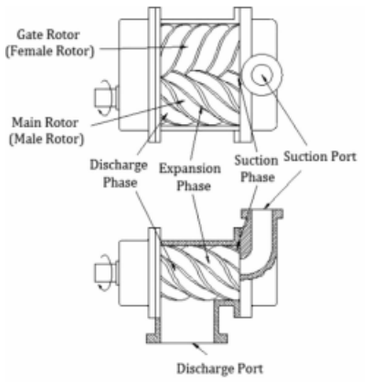

Figure 9: Working principle and components of screw expander [20]

5.4.3 Scroll Expander

Scroll expander is formed by a stator and a rotor with spiral shape. The high pressure fluid makes the rotor move around the stator eccentrically transforming work. The scroll expander are widely used in industry and their simplicity makes them cheap [5]. They can operate until 180 °C and 8.2 MPa. Quoilin et al., [10], have studied the efficiency of scroll expanders evaluating boiler temperature, mass flow, rotational speed of the expander and its isentropic efficiency for ORC and it showed expander efficiency from 42 % to 68 %. The highest isentropic efficiency achieved for a scroll expander was from 83 % according to Imran et al [20],. Two types of leakages can be found on scroll expanders when operating at low speed, flank and radial leakages. Radial leakage is caused by the clearance between top and/or bottom plate and the scroll whereas flank leakage path occurs due to clearance between flanks and scroll [20]. The following figures 10 and 11 shows the architecture of a scroll expander as well as the two types of leakages [21, 20].

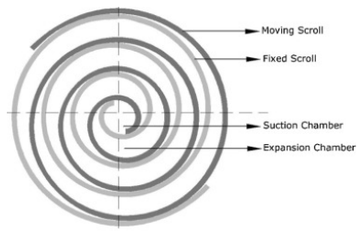

Figure 10: Scroll expander working principle and architecture [21]

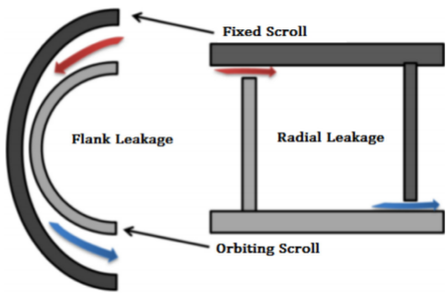

Figure 11: Scroll expander leakages [20]

5.4.4 Piston expander

Piston expanders are commonly used in waste heat recovery systems from internal combustion engines as well as for refrigeration. The average efficiency of the piston expander is about 50 % although a maximum efficiency of 76 % has been reported in other papers. Piston expanders are characterized by a lower rotational speed, from 600-2000 rpm, compared to screw and vane expander. This characteristic eliminates the need of a speed reduction gearbox [20]. Their maximum power output is rather low, less than 2 kW. As will be seen in the *Results* section, the power output of the system varies from around 600 kW to approximately 2 MW. This relatively high NPP output makes the piston expander impractical for this installation.

To conclude, in ORC system units for WHRS will use different expanders depending on the heat source used. For recovery systems using exhaust gases as heat source a dynamic expander

will be more suitable, specifically a turbine with an axial flow disposition. On the other hand, as ORC powered by jacket water have a lower power output, volumetric expanders and radial-flow turbine will be more adequate [2].

5.5 Working Fluid selection

In this section, the selection of the working fluid will be discussed. Working fluid selection is a decisive parameter in order to get the higher thermal efficiency. Also it is a crucial selection to use the heat source in a optimum way. Besides, in the ORC working fluid selection, other factors such safety and technical feasibility has to be taken into account [22]. Some important characteristics for the working fluid are low-toxicity and non-flammable, as in case of some leak to avoid any accident in the vessel. Also, it has to be non-corrosive, to avoid corrosion in the components, e.g., plumbing installation, pumps, HEx [7]. Specially for the turbine component as during the expansion in some cases the steam quality of the working fluid in the outlet is not 100 % in all cases. This will imply that in the outlet of the turbine some drops of the fluid will be formed due to the expansion process and this can cause several damage in the blades of the turbine, implying costs in repairing the expander.

Organic fluids can be classified as wet, dry and isentropic fluids. This classification is based on the dT/ds of the saturation vapor curve. Fluids that have a negative saturation vapor curve, $dT/ds < 0$, are classified as wet fluids. Nevertheless, when an organic fluid has a $dT/ds > 0$ it is called dry fluid. Lastly, when $dT/ds = 0$ the organic fluid is isentropic. In Figure 12 shows the different saturation vapor curve of the different organic fluids mentioned above [23].

Rankine cycle is normally powered using water as working fluid in the well-known SRC. Water is a wet fluid, however, to avoid condensation in the last stage of the turbine, superheating is required. Also, a minimum inlet temperature of 450 °C is required in the turbine inlet to avoid droplets formation [7] and [23]. Turbines that operate using steam are also rather expensive due to their complex design. Because of all this working conditions, water as well as wet fluids are more suitable for high-temperature application, therefore, for this rather low-temperature application they will be discarded [23].

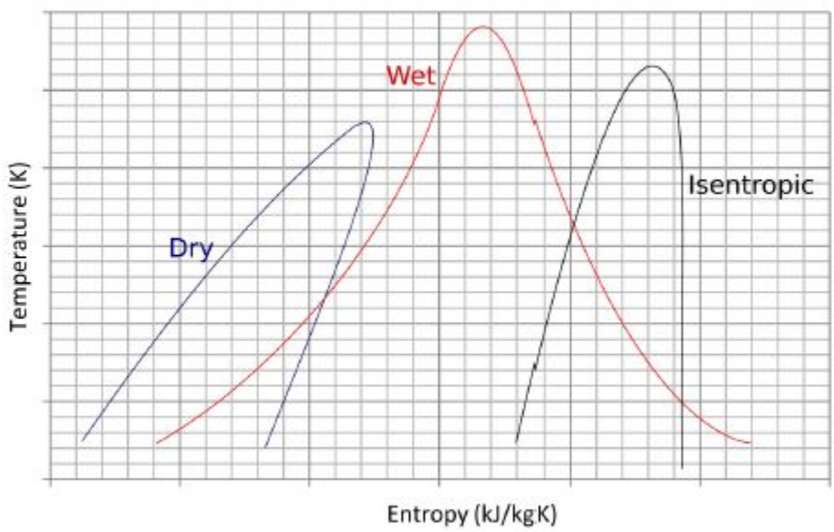

Figure 12: T-s diagram of dry, wet and isentropic fluids [23].

In respect of thermodynamics properties, organic fluids with high latent heats, low specific heats and high densities will be preferable [23]. Working fluids with low density implies higher volume flow rate. This will affect to the size of heat exchanger making them bigger to avoid pressure drops, therefore the installation will end up being more expensive [10]. On the other hand, low specific heat and high latent heat will help in terms of heat transfer of the system, i.e., leading to lower areas required in the heat exchangers.

Organic fluids can also be classified by their chemical composition [23]:

- **CFCs**. Chlorofluorocarbons. They care composed by carbon, fluorine and chlorine. Also known as 'Freon'. Some examples are R11, R12, R13, R113, R114 and R115.

- **HCFCs**. Hydrochlorofluorocarbons are composed by carbon, chlorine, fluorine and hydrogen. Such type of organic fluids are R21, R22, R123 and R124.
- **HFCs**. Hydrofluorocarbons. They contain carbon, hydrogen and fluorine. There is a considerable list of HFCs, however, for this project R134a and R152a will be used as working fluid for some configurations.
- **PFCs**. Perfluorocarbons. Also they are called fluorocarbons and they are composed only by carbon and fluorine. There are two organic fluids in this group. R14 and R116.
- **HCs**. Hydrocarbons. They contain carbon and hydrogen atoms. These are known by the name of Ethane (R170), Propane (R290), Butane (R600), Pentane (R601), benzene, toluene and cyclohexane.

CFCs, chlorofluorocarbons, and HCFCs, hydrochlorofluorocarbons, have been used as refrigerants. They are characterized for having a rather high safety in terms of operation and handling. CFCs, were banned because they were characterized for having a hihgh global warming potential (GWP), after the prohibition, CFCs were replaced by HCFCs [23]. Even so, HCFCs were substituted by HFCs as these do not contain chlorine and they do not affect to the ozone layer but they also have a high GWP.

Hydrocarbons, HCs, like Propane (R290), Butane (R600) and Pentane (R601) are widely used in refrigeration as well as in ORCs. They have superb thermodynamic properties, better than other HCFs and HCFCs. They also can be considered environmentally friendly for this application as they have zero Ozone depletion potential, ODP, and quite low GWP. Nevertheless, they are highly flammable so they have to be carefully handled. They can represent also a explosion risk if the concentration of HCs is inside the lower and upper flammability limits [23]. Besides, for cycle temperatures around 350 ºC, hydrocarbons are suitable due to their thermal stability [7].

The evaporation temperature of the organic fluids will be also one of the working fluid parameters selection. As in the following section will be commented, the system will be modelled fixing to pinch points and then selecting the minimum of the ORC massflow. After some simulations, working fluids with lower evaporation temperature led to higher temperature difference between the inlet of the evaporator and outlet of the evaporator. However, this will be discussed with more detail in the following sections. The following Table 1, shows the different properties of the working fluids chosen for this project. Environmental aspects will be measured using ODP and GWP factors. The ODP measures the relative degradation of each fluid using R11 as a reference fluid. The ODP for R11 will be 1. ODP values under 0.1 are considered medium and above 0.1 it will be say that they have a high ODP. Global Warming Potential, GWP, measure how much heat from the fluid gases gets trapped in the atmosphere compared to the heat absorbed by an identical amount of CO_2 calculated in the interval of 100 years. GWP values under 150 are considered low, values between 150-2500 will be considered medium whereas values over 2500 will be estimated as high [23].

ASHRAE Code	Latent Heat of Evaporation at 0.1 MPa [kJ/kg]	Critical Temperature [K]	Critical Pressure [MPa]	Type of Fluid	ODP	GWP-100 yr
R134a	217.16	374.21	4.0592	Isentropic	0.055	1430
R152a	330.18	386.411	4.5167	Wet	0	124
Pentane	357.89	469.7	3.37	Dry	0	4
R123	170.35	456.831	3.6618	Dry	0.02	77
R113	144.45	487.21	3.3922	Dry	1	6130

Table 1: Characteristics of the working fluids selected for this project [23].

6 Modelling of the ORC system

The different configurations of the ORC installation inside the vessel will be discussed. The program used for the modelling and simulation will be EES, Engineering Equation Solver. The heat source used for the three of them will be the exhaust gases of the 8S70ME-GI engine with low pressure SCR tuning, which power output is from 23 MW. The inlet of the exhaust gases will be at a temperature of 532.2 K and their massflow will be equal to 49.1 kg/s, lastly they will be characterized for a specific heat of $c_p = 1.06 kJ/kg \cdot K$. In this thesis, there will be also a steam

production requirement, that will use as well the exhaust gases as a heat source and they will flow through a HRSG. The steam massflow will have two reference value of high and moderate steam requirement of 1730 and 865 kg/h of saturated steam a 7 bar respectively. The influence of the steam production will be studied as well for the arrangements that will show dependence on the HRSG requirements.

For this project, three different configurations will be studied and they will be explained more detailed in the following subsections. During the simulation, some parameters like inlet turbine pressure will be varied to see the behaviour of the system doing a sweep from a lower value until getting close to the critical pressure of each fluid. Some basic constants will be assumed for the modelling such as condensing temperatures and pinch point. The efficiency of the turbine as well as the efficiency of the pump will be fixed for the three different layouts. A value of $\eta_{p,t} = 0.85$ will be assumed as it is a typical value found in some problems related to Rankine cycle. An inlet temperature of 30 ºC (303,15 K) for the organic fluids will be assumed. This value is not a random value. When the different working fluids were selected, their respective diagrams were used to see if this temperature gave a reasonable outlet pressure value for the turbine, besides, as the cold source for the condenser is seawater, it was not possible to cool the different organic fluids to lower temperatures. Moreover, values of the steam quality were fixed in the outlet of the condenser, x_1, and for the inlet of the evaporator, x_3, as 0. For the outlet of the ORC boiler, x_5, a value of 1 was also fixed. Regarding the superheating value, for the five different organic fluids was optimized and a value of $dT_{sup} = 1$ was assumed for the three configurations and for all the different working fluids. The three different configurations will be commented in detail.

6.1 Configuration I.

The layout of the first configuration will be described in this section. In this configuration, the exhaust gases flow first through the HRSG, and afterwards, the remaining heat will be used in the ORC boiler. First of all, the different stages of the steam were calculated. Considering an inlet temperature of 50 ºC for the water, the different enthalpy and temperatures of the steam are calculated to know the hot side outlet temperature of the HRSG. Table 2 shows the different state points of the steam through the steam generator. Lastly, the heat transferred in the HRSG will be calculated using the difference of temperature of the exhaust gases in the HRSG part using the following expression.

$$\dot{Q} = \dot{m}_{exh} \cdot c_p \cdot [T_{inl} - T_{out}] \tag{1}$$

Point	**Pressure [bar]**	**h [kJ/kg]**	**T [K]**
1	1	209.3	323.2
2	7	697.3	438.1
3	7	2763	438.1

Table 2: Steam states during the HRSG.

Figure 13 shows the Q-T diagram of the HRSG. As can be seen, the outlet temperature of the exhaust gases decrease when the steam requirement increase. This is because the heat required increases with the steam requirement, making the temperature at the outlet of the HRSG lower and, therefore, the available heat in the ORC boiler will decrease as well. To simplify the figure, the transferred heat axis, i.e., $\dot{Q}$, has not any value as what is being represented here is how the exhaust gases temperature varies depending on the steam requirement.

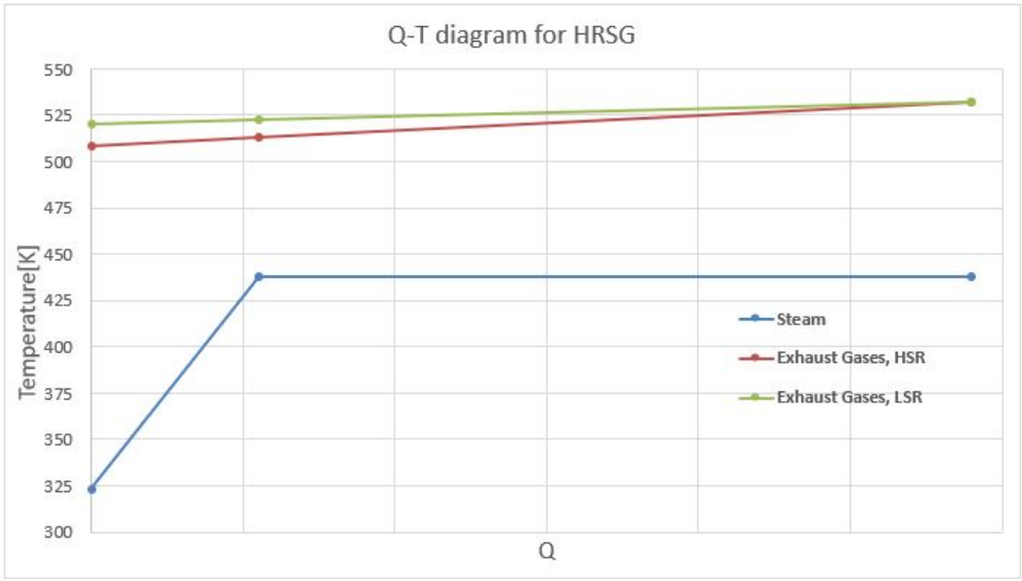

Figure 13: Q-T diagram of the HRSG

Once the exhaust gas temperature after the steam generation process is known, the different states of the ORC will be calculated. First, the inlet temperature as well as the pressure of the fluid, the degree of superheating in the ORC boiler and the different steam qualities throughout the ORC system are defined. It has to be commented again to clarify that the pressure will be increased in 5 bar interval until achieving the critical pressure of the fluid during the simulations. The temperature of the turbine inlet will be calculated by assuming that it will be the same as in the outlet of the superheating of the ORC boiler.

$$T_{inl,expand} = T_{out,boil} \tag{2}$$

And $T_{out,boil}$ will be calculated after knowing the temperature of the selected fluid at the selected pressure, once it has been fully evaporated and, then, superheated.

$$T_{out,boil} = T_{evap} + dT_{sup} \tag{3}$$

To calculate the enthalpy outlet of the turbine, the different entropy state of the turbine is required. First, an isentropic state will be assumed to calculate the outlet enthalpy assuming that the expansion process has been isentropic and with the entropy in that point, the ideal value of the enthalpy after the expansion will be calculated. Then, the real outlet enthalpy is calculate through the efficiency equation of the turbine showed below.

$$\eta_t = \frac{h_{inl} - h_{out}}{h_{inl} - h^s_{out}} \tag{4}$$

Once the fluid has been expanded, it flows through the condenser where it comes back to its liquid phase. Afterwards, the fluid will go throughout the pump. The procedure to calculate the working fluid state after the pump is similar as the one used for the turbine outlet. An isentropic state is assumed in the outlet of the turbine, then the ideal outlet enthalpy of the pump is calculated through EES. Finally, a real outlet enthalpy is calculated through the pump efficiency formula.

$$\eta_p = \frac{h^s_{out} - h_{inl}}{h_{out} - h_{inl}} \tag{5}$$

For the different phases in the ORC boiler, i.e., pre-heater, evaporator and superheater; the multiple states will be calculated setting the outlet pressure of the pump and steam quality at each point. Once the different points of the ORC cycle has been calculated, the massflow of the system will be calculated. First, a pinch point of 15 K will used for the calculations. As commented in section 5.1.1, an optimum value from 15 to 20 K of pinch point for an internal combustion engine can increase the efficiency up to 7% of the system [18]. The pinch point will be set at the beginning of the evaporation phase and in the outlet of the ORC boiler. Once the pinch point value has been fixed, two energy balances will be used to calculate the massflow of working fluid. One will be set between the inlet and the outlet of the system and the other will be set between the inlet and before the evaporation phase in the ORC begins. Then the minimum from both of the massflow will be selected. The unit was modelled in this way because for some working fluids, when the massflow was calculated only taking into account the pinch point after the pre-heating phase, for

some cases the program converged in solutions where the outlet of the exhaust gases was not real in thermodynamic terms, i.e., the exhaust gases were colder than the ORC in some points of the pre-heating phase. In this way, for some working fluid, the pinch point of the evaporator was rather high but guaranteed the proper functioning of the model.

Once the massflow of the system have been calculated, the different temperatures of the exhaust gas through the ORC boiler will be calculated following some different energy balances. The energy balances will be calculated as following.

$$\dot{m}_{exh} \cdot c_p \cdot (T_{inl,ORCboil} - T_{calc}) = \dot{m}_{ORC} \cdot (h_{out,boil} - h_{calc}) \tag{6}$$

Where T_{calc} and h_{calc} are the state where the temperature of the exhaust gas has to be calculate, i.e., the different temperature differences along the boiler. The last calculation carried out in this configuration was the power output of the ORC. Firstly, the pumping power consumption and the turbine power was calculated using the following expressions.

$$\dot{W}_{pump} = \dot{m}_{ORC} \cdot (h_{out} - h_{inl}) \tag{7}$$

$$\dot{W}_{turb} = \dot{m}_{ORC} \cdot (h_{inl} - h_{out}) \tag{8}$$

And lastly the net power production of the system was calculated as the substraction of W_{pump} to the power generated by the turbine, W_{turb}.

$$\dot{W}_{net} = \dot{W}_{turb} - \dot{W}_{pump} \tag{9}$$

To conclude, a diagram of the first configuration is shown by Figure 14.

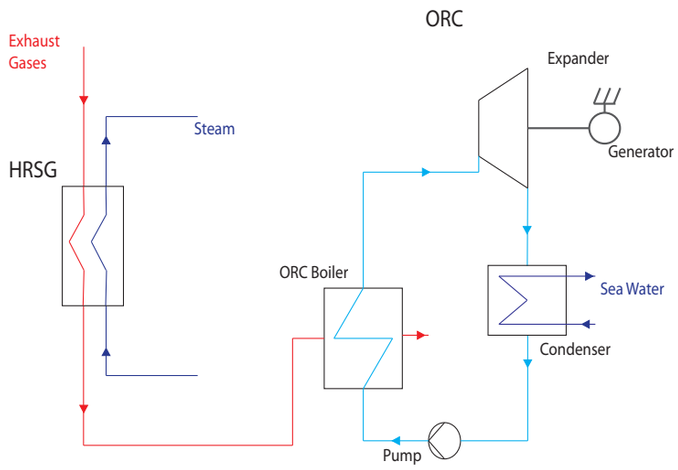

Figure 14: First configuration of the implementation of the ORC system.

6.2 Configuration II.

The characteristics of the second configuration will be discussed. In this second layout, the exhaust gasses flow firstly through the ORC system and once the exhaust gases have flowed through the ORC boiler, they will move to the HRSG as it is shown in Figure 15.

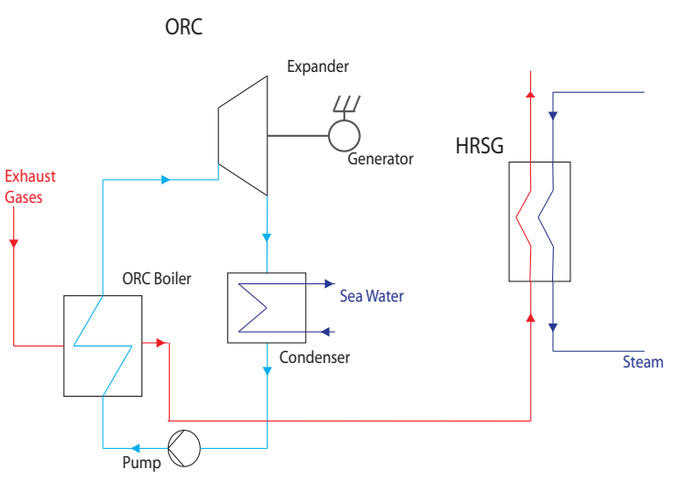

Figure 15: Diagram of the second configuration of the system.

This configuration represented a design problem as the steam generation needed a minimum temperature to be produced. As the only data known of the exhaust gases are the mass flow and the inlet temperature, some suppositions will have to be done. First, the different temperatures of the steam can be seen in Table 2. Once the evaporation temperature of the steam at 7 bar is known, a pinch point of $\Delta T_{pp} = 5K$ will be assumed. Reducing the pinch point to a rather low value will decrease the exergy loss in the HRSG and also after some trials, the ORC power output increased as well when using a lower pinch point for the HRSG. Once this temperature is known, an energy balance is set between the exhaust gases and the inlet to calculate the inlet temperature of the exhaust gases in the HRSG as well as the outlet temperature of them.

Once the required temperature at the inlet of the HRSG is calculated, the available heat for the ORC boiler will be the difference between the inlet temperature of the exhaust gases, 532.2 K, and the inlet of the HRSG. This second parameter will vary depending on the steam requirement of each case. In this second configuration there will be only used the organic fluids whose evaporation temperature are higher. In this way, the pinch point difference between the exhaust gases and the organic fluid will be more feasible. Otherwise, for fluids with relatively low evaporation temperature values will end up with high mass flows that will be discarded as the mass flow calculation is the same as in the previous configuration. The different states of the fluid in the ORC system will be calculated as mentioned in section 6.1 as well as the pinch point in the organic fluid boiler. Lastly, the power calculations have been calculated following also the same expression of energy balances that have been explained in the previous section.

6.3 Configuration III.

For the third configuration, the total massflow of the exhaust gases will be split in two. During the simulations, different variations in the amount of exhaust gases that are sent to the ORC system to see its performance and how the ORC power output varies with the quantity of exhaust gases sent to the system. For this configuration, not all the working fluids will be used as it has been done in the first one. The reason of this selection of few organic fluids is because in this layout, the exhaust gases inlet temperature to the ORC boiler is rather high, compared to the first configuration where first, the exhaust gases flows through the HRSG and then, they flow to the ORC boiler. This high temperature will lead for fluids like R134a that have a relatively low boiling temperature, even at high pressures, that the massflow calculated for the case where the pinch point is set before the evaporator, had an incredibly high value , around 80 to 110 kg/s, therefore, the EES code ended up taking the second massflow because it was smaller. In this second calculation, the pinch point was set at the inlet of the ORC boiler, or outlet for the exhaust gases, having even higher values of pinch point compared to the first configuration. To avoid this behaviour only three working fluids will be used. The combinations used for the third configuration were, 50%-50%, 60%-40%, 70%-30%, 80%-20%. Where the first number correspond to the total percentage of exhaust gas massflow sent to the ORC boiler. The different state points of the ORC will be calculated as in section 6.1 as well as the massflow, the different pinchpoints and the power calculations. The values, as expected, will be varying depending on the fluid as they have their own properties, but as well as for the first configuration, there will be a pressure sweep for all the fluids and for the different combinations of mass flow distribution. Figure 16 shows a diagram of the third configuration where the exhaust gases are split.

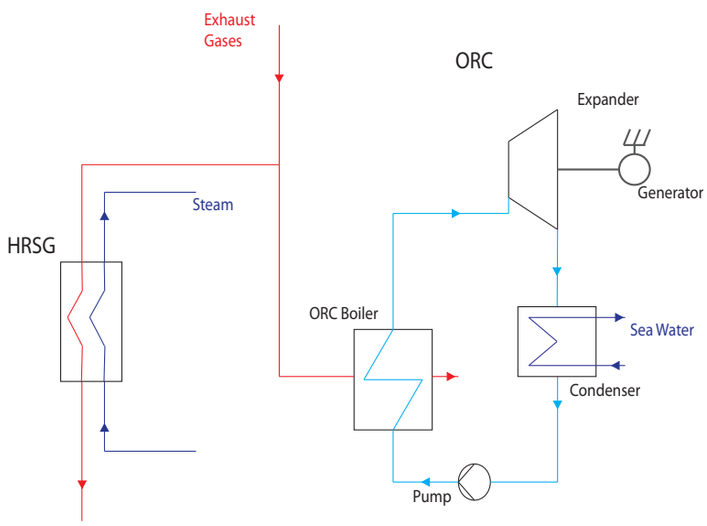

Figure 16: Diagram of the Configuration 3.

7 Results and discussion

In this section the different results for the three configurations will be studied. Lastly there will be a study of how the influence of steam requirement influences on the power production, compared to a theoretical model where there is no steam production at all, meaning that all the heat from the exhaust gases goes directly to the ORC cycle. Three main parameters that will be studied. Net power production, thermal efficiency and pinch point in the ORC boiler. Also there will be some brief comments about the massflow through the ORC system but as it has been modelled to be a dependent parameter of the pinch point, in this review, there will not be given much relevance as during the simulations the amount of massflow was carefully controlled to not have excessive high values for the system.

7.1 Results for Configuration I.

Configuration I was planned as to be the reference of the project. All the numerical results for the first configuration can be found between Tables 1 to 10 in Annex I. In Figures 17 and 18, NPP is displayed for the different working fluids used in the simulations. As can be seen there is a tendency to increase the power output as the pressure in the turbine is augmented. This is because as the pressure is increased, the enthalpy of the fluid increases too, so, as the expansion gets to the same value of pressure, i.e., the outlet pressure of the turbine is for each fluid their correspondent depending the pressure calculated depending the saturation pressure after the condenser, the enthalpy drop increases as the pressure increases, making the power of the turbine higher and in consequence, the NPP increases too. Though, there are some fluids that seem do not follow that trend. R113 seems to decrease the NPP after 10 bar. This behaviour could be explained by the steam requirement, for LSR. In Figure 18, R113 seems to increase slightly the power production for higher pressures when the HRSG does not require a high steam production. However, when R113 is simulated with high pressures, the solution converges when the pinch point is set in the evaporator, this makes the massflow of the working fluid decrease, decreasing power output too because it depends on the massflow of the working fluid, see Tables 9 and 10 from Annex I. Besides, R113 has the lower latent heat. Lower latent heats will represent lower power outputs [23]. Lastly, R113 shows lower output temperature of the EG, Tables 9 and 10 from Annex I, compared to the other fluids, supporting that the heat absorbed by the ORC boiler is smaller and, therefore, less thermal energy is harvested. Pentane, seems to behave the same way for HSR, and their outlet temperature from the exhaust gases is higher than the other organic fluids. See Table 5 from Annex I.

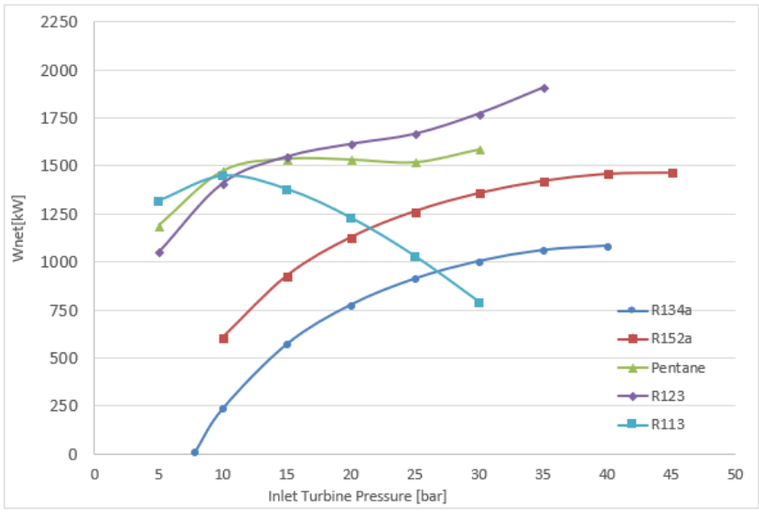

Figure 17: Net Power Production of the ORC when the system is operating with Configuration I for HSR.

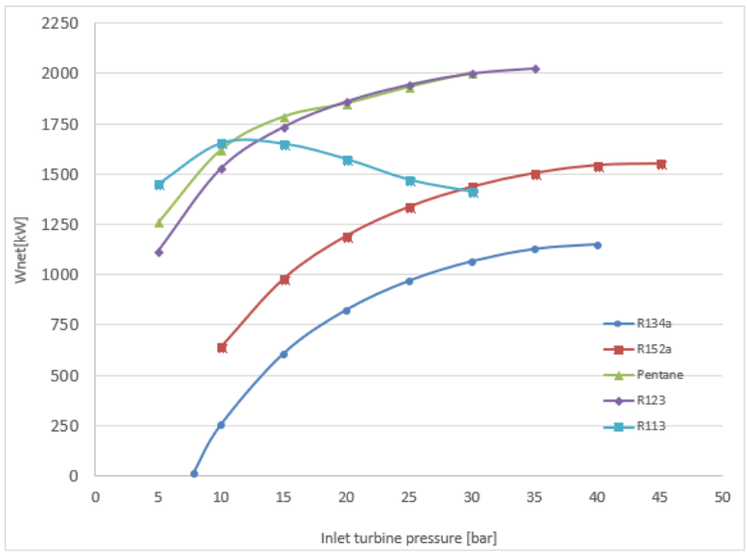

Figure 18: Net Power Production of the ORC when the system is operating with Configuration I for LSR.

Figure 19 shows the thermal efficiency for different working fluids in the Configuration I. Thermal efficiency seems to increase with the increment of pressure, see Tables 1 to 10 from Annex I, therefore, it can be stated that the higher the pressure, the better the ORC system harvests the remaining heat from the exhaust gases after flowing through the HRSG. Also it has to be commented that the efficiency does not seem to be affected substantially by the steam requirement, hence, an average value will be used to represent the thermal efficiency of the system with the first configuration as the variation is not large enough. The thermal efficiency will be calculated as following.

$$Efficiency[\%] = \frac{\dot{W}_{NET}}{\dot{Q}_{ORC,boil}} \tag{10}$$

R113, R123 and Pentane have higher thermal efficiency compared to R152a and R134a. The selected pinch point for the system seems to affect to the efficiency of the system, the highest efficiency are shown in those fluids that after the EES simulation , they have converged in solutions where the pinch point in the evaporation, point 3 in the different Tables 5 to 10 in Annex I, is 15 or close to 15. As commented before, a pinch point between 15 and 20 K at the beginning of the evaporation can increase the system efficiency [18]. For most of the cases, when the system was using R113 and Pentane the solution converged setting the pinch point after the preheating phase. R123 model, for LSR, sets always the pinch point in the outlet, see Table 8, but the pinch point before evaporation keeps rather low values, around 20-25 K.

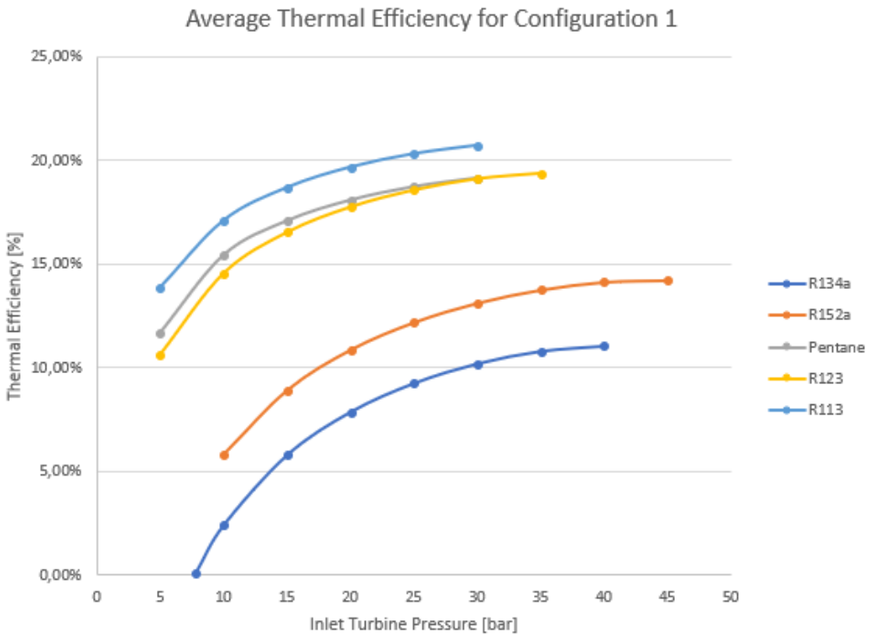

Figure 19: Average Efficiency of the ORC system when it working with Configuration I.

7.2 Results for Configuration II.

In this section, the results obtained from Configuration II will be commented. For this layout, a reduction in the power output will be expected as there are some restrictions in the heat transferred to the ORC system due to there has to be enough heat for the HRSG. Also, as commented before, to try to reduce the maximum the pinch point at the evaporator, the fluids with their highest evaporation temperature will be selected. For R134a and R152a their pinch point was somewhat high and their power output was comparably low to the other fluids. In any case, for this configuration, higher pinch points are expected due to the restrictions of the heat source.

Figure 20 and Figure 21 shows the power output for the different fluids. Tables 11 and 12 in Annex I shows the results for Pentane in Configuration II. As can be seen, $\dot{m}_{ORC}$ is relatively low compared to the other two fluids for Pentane. Even so, Pentane has a similar power output compared to the other two fluids. This is because of its latent heat. If the latent heat of a fluid is higher, they will provide also higher work output during its expansion [23]. On the other hand, the massflow of the R113 is rather high compared to the R123 massflow for high pressures, see Table 13 to 16 in Annex I,this will make that, even though they have similar latent heat, this difference in $\dot{m}_{ORC}$ makes the power production to increase.

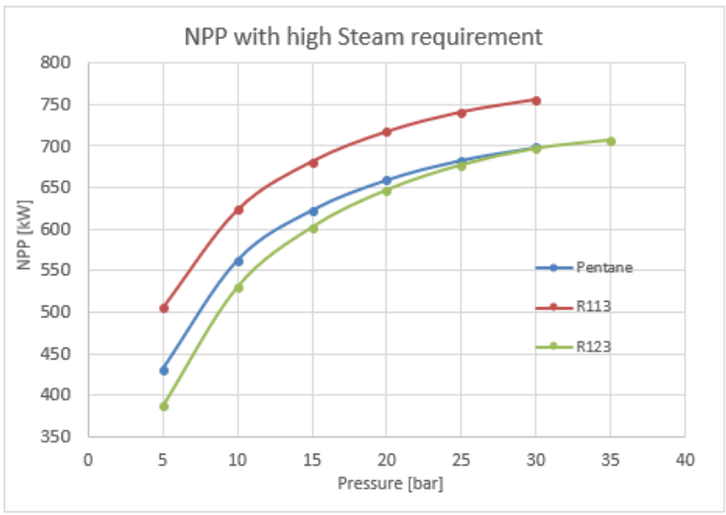

Figure 20: Comparison of the NPP for all the working fluids when are operating under HRS for Configuration II.

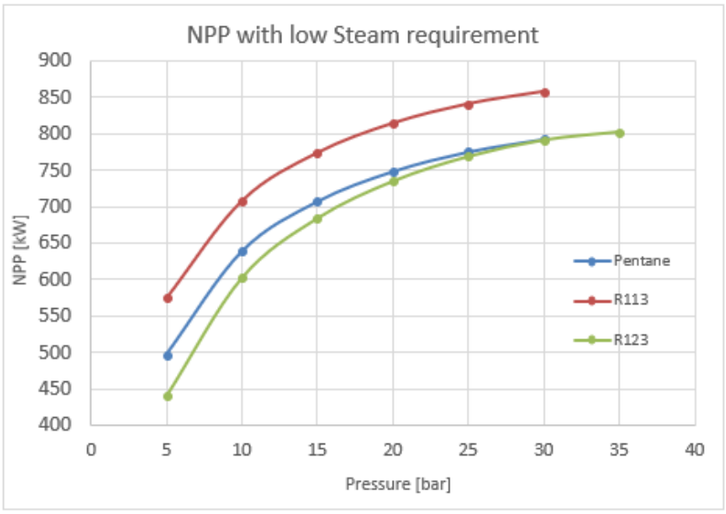

Figure 21: Comparison of the NPP for all the working fluids when are operating under LRS for Configuration II.

Figure 22 shows how NPP variation for each fluid depending on the inlet turbine pressure and the steam requirement for each of them. As predicted, higher pressures lead to higher NPP output. Also, when as the steam requirement decreases, the NPP increase. A decrement of the steam requirement will mean that the outlet temperature of the ORC system will decrease as well because less heat for the HRSG is needed.

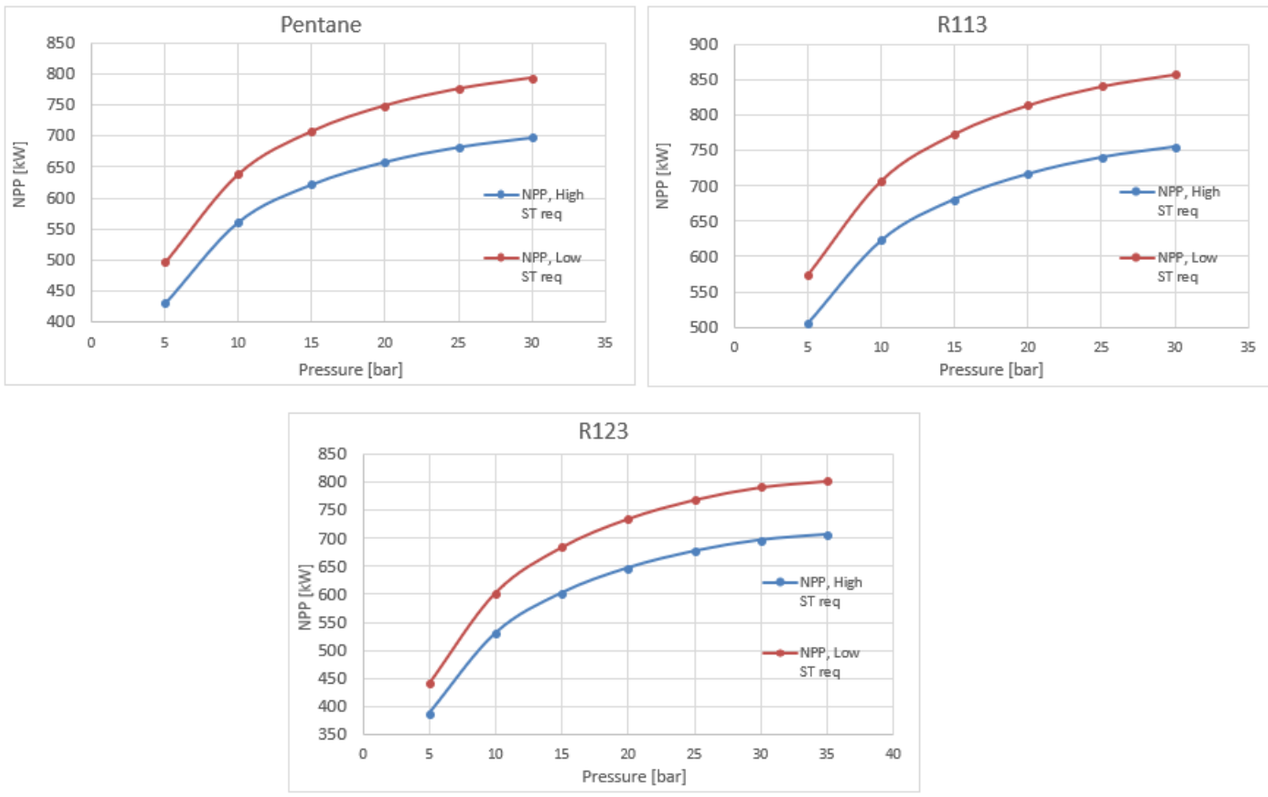

Figure 22: Net Power Production of the ORC for Configuration II for the different working fluids selected.

Thermal efficiency increases as the pressure is increased for Configuration II. This is because a combination of two factors. As the amount of heat used in the boiler each case is the same because of the steam requirement restrictions, the increment of power output will increase the thermal efficiency consequently. Also, as the pinch point decrease with the pressure because the evaporation temperature increase, the thermal efficiency increases as the heat is harvested in a better way in the ORC boiler.

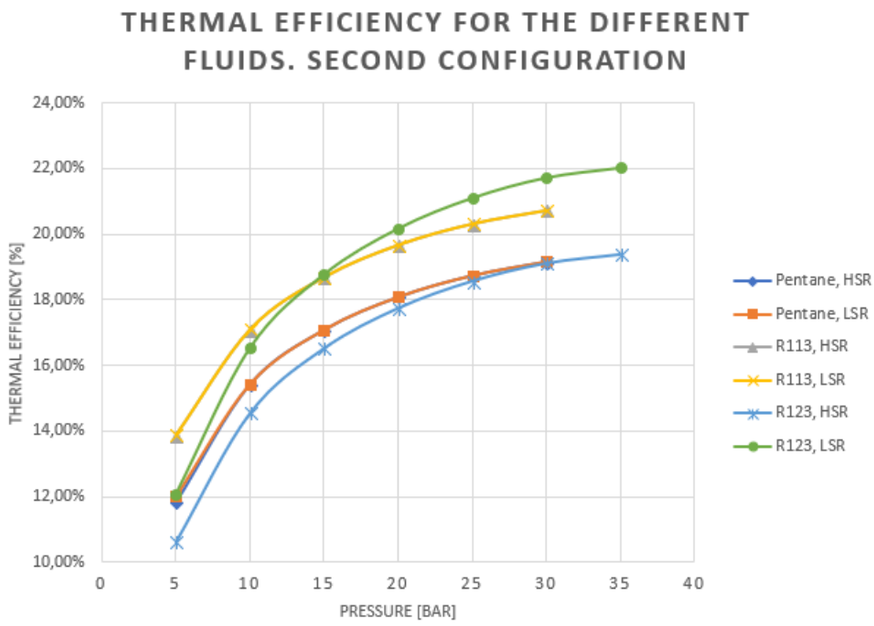

Figure 23: Average Thermal Efficiency for the different working fluids operating with Configuration II.

For the working fluid that showed the lower pinch point at high pressure, a comparison between the pinch point and the efficiency of the system will be shown in Figure 24. This was for R113 when the steam requirement was of 865 kg/h, i.e., low steam requirement. As can be seen, the decrease of the pinch point increases the thermal efficiency substantially.

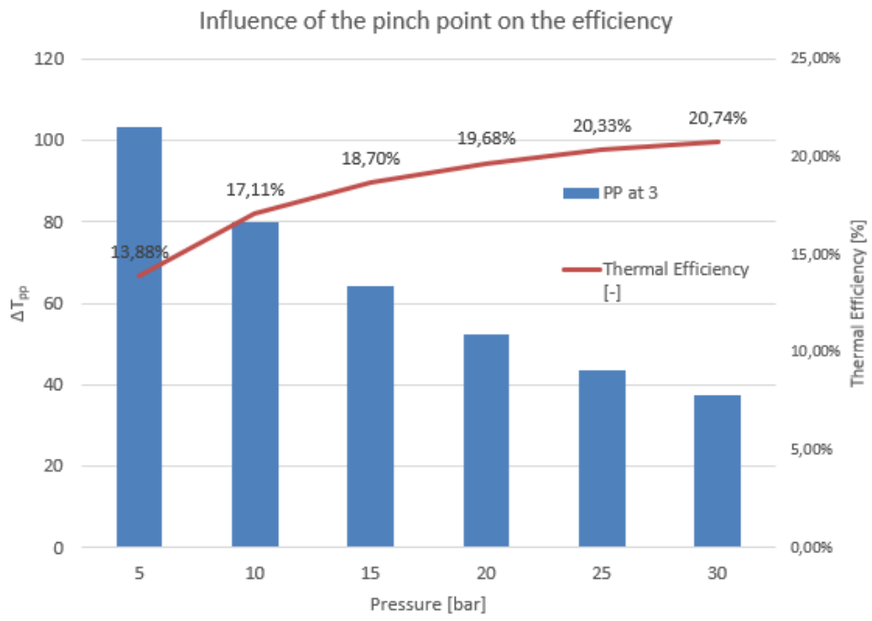

Figure 24: Influence of the pinch point on the ORC.

Figure 25 depicts the variation of the pinch point for the three different working fluids and both steam requirements. As seen, the pinch point tends to decrease as the pressure increase due to the increment of the evaporation temperature. Then the difference between the heat source and the working fluid at the outlet of the evaporator, i.e., the pinch point, is reduced.

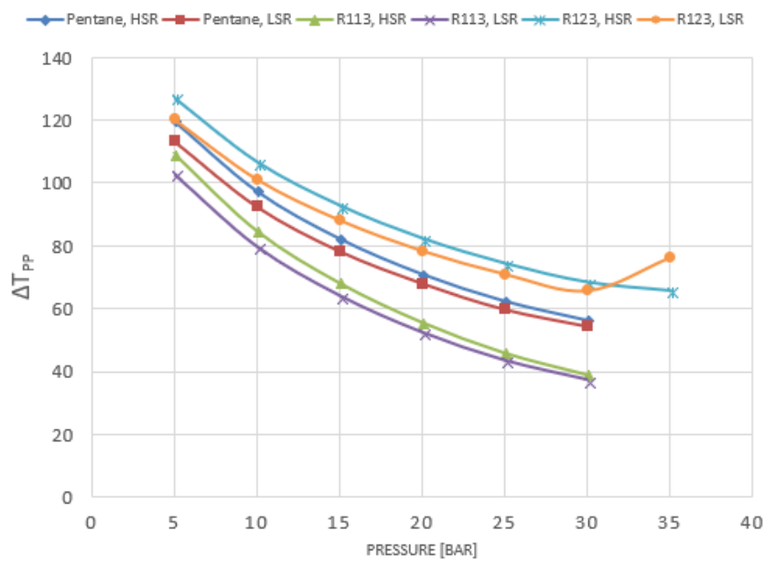

Figure 25: Pinch point variation of the system using Configuration II.

7.3 Results for Configuration III.

In the third configuration, the massflow from exhaust gases was split. The EES model used during the simulations showed that, when changing the amount of exhaust gases used in the ORC system, the massflow of ORC was changed consequently to keep the pinch point restrictions of the system, meaning that the inlet and outlet temperature of the exhaust gases did not changed with the increment of exhaust gas massflow, but, the temperature along the evaporation phased did changed. This results can be seen in Tables 16-26 in Annex I.

Figure 26 shows how the net Power production varies depending the percentage of working fluid sent to the ORC system. On the other hand, Figure 27 depicts how this increment of the of massflow in the exhaust gases affects to the heat recovery system for the fluids separately. As can be seen, an increase in the amount of massflow sent to the ORC system increases the power output as expected. The augment of massflow represent an increase in the availability of the heat from the EG that can be harvested. Also the NPP seems to increase with the pressure as the expansion in the turbine increases. Pentane and R123 have the highest NPP when the system is

working at high pressures. R113 and R123 seems to show some anomalies during the simulation as can be seen in the different peaks of NPP shown in Figure 26 and Figure 27.

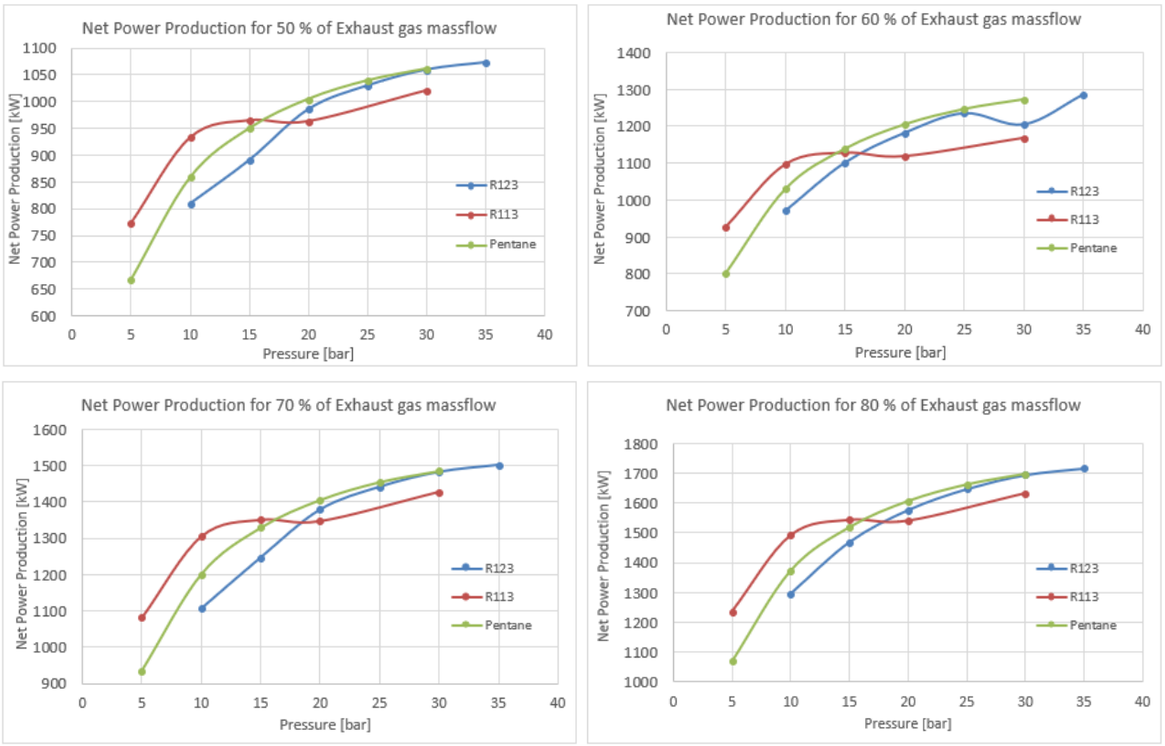

Figure 26: Net Power Production for the third configuration, with different percentages of exhaust massflow.

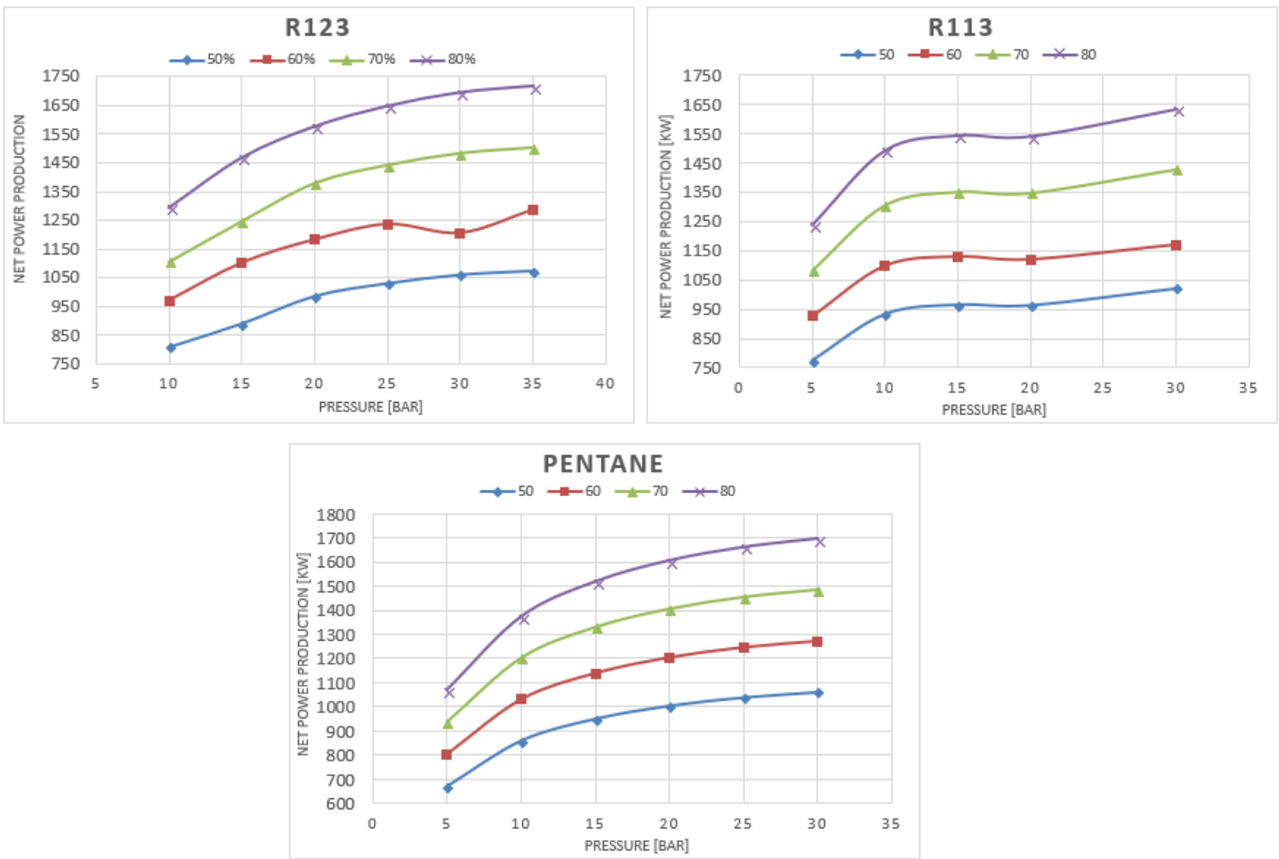

Figure 27: Comparison for each different fluid when the amount of exhaust gases is varied.

The efficiency seems also to increase with pressure according to Figure 28. This is because the power produced by the system increases as well due to the gain of $\dot{m}_{ORC}$. R113 is the fluid with the highest efficiency whereas Pentane and R123 has similar average values. Tables 16 to 19 from Annex I shows the result for the third configuration when the system is using R123 as working fluid. As the results shows, the system does not set the pinch point at '3', that is the point before the evaporation begins in the ORC boiler, because as commented in the previous section, the

model picks the configuration that has a lower $\dot{m}_{ORC}$. The same behaviour is seen for Pentane, see Tables 23 to 26 in Annex I. Accordingly, even their pinch point at 3 is rather low, they never have the lower value, set as 15 K, this makes the thermal efficiency relatively lower compared to R113.

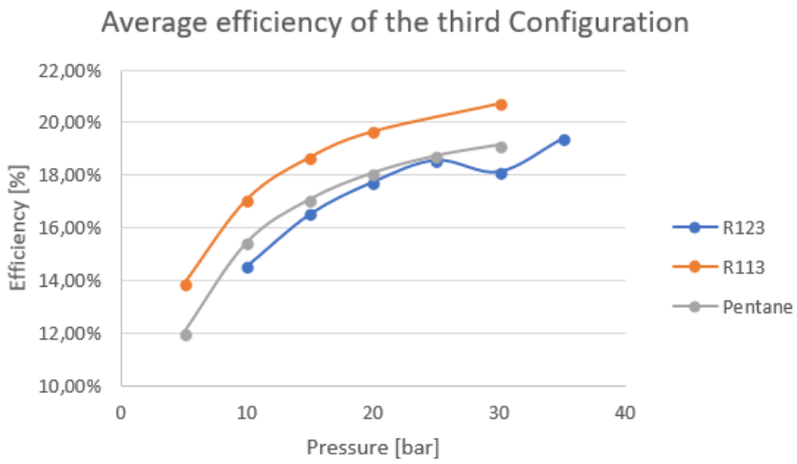

Figure 28: Average efficiency for the ORC system for the Configuration III.

7.4 Influence of the Steam Requirement between configurations compared to the maximum power assumption.

A maximum power output of the ORC system will be assumed. For this theoretical model, all the EG will flow through the ORC model. A pressure of 30 bar will be assumed for all the fluids as it is a value common for all the 5 fluids. Also, when the fluids are compressed until 30 bar they show relatively high efficiency and power output. The second and third configuration will be also tested using R134a and R152a, even though they have showed high pinch point temperatures. The maximum output will be represented as a straight blue line because there is no steam production on it. Configuration III does not show influence over the steam requirement. This is because these are two independent process and the distribution of exhaust gas will be lead only to lower temperature outlet of the exhaust gases for the HRSG. Figure 29 shows the influence the performance of the ORC system depending the configuration for the five different working fluids at 30 bar.

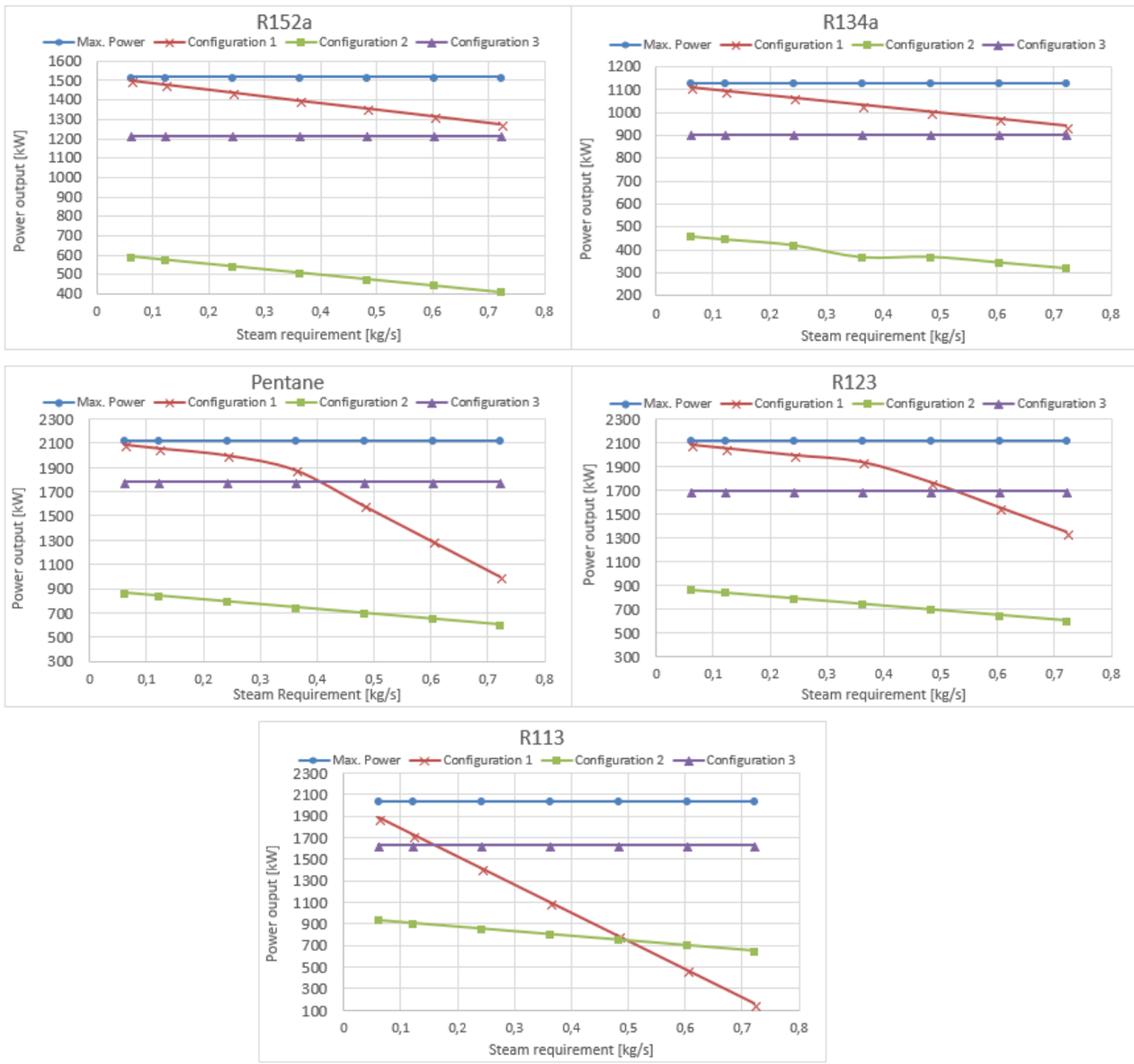

Figure 29: Behaviour of the ORC system for the three different configurations.

For R134a can be seen that the best configuration that can be used is configuration 1. Even so, if the steam requirement keeps increasing probably the third configuration will be better for the system. However, the maximum steam requirement used for this assumption is 0.72 kg/s, 2600 kg/h approximately. This is a rather high steam requirement. R152a shows the same tend as R134a. For both fluids, the second configuration, has the lowest power output.

R123 also shows that the worst configuration is configuration II in terms of NPP. This decrease in power output for all the fluids is because the restriction of inlet temperature of the HRSG, causing a decrease in the heat available for the ORC boiler. However, R123 shows that for high steam requirements, i.e. values over 0.5 kg/s, the third configuration will produce more power output compared to the first configuration and, as expected, compared to configuration 2. Pentane, on the other hand, shows a behaviour similar to R123. Also, Configuration II shows the lowest power production.

If R113 is used as a working fluid, it shows a clear decrease for Configuration I when the steam requirement is increased. Third configuration shows for the all the cases complete stability although for low to medium steam requirements the power output is rather low compared to the first configuration. To conclude, the temperatures along the HRSG depending the configuration and the reference steam requirement will be shown in Table 3.

Configuration I			
		$T_{HRSG,inl}[K]$	$T_{HRSG,out}[K]$
HRS		532,2	508,6
LSR		532,2	520,4
Configuration II			
		$T_{HRSG,inl}[K]$	$T_{HRSG,out}[K]$
HRS		462,2	438,9
LSR		452,7	440,9
Configuration III			
		$T_{HRSG,inl[K]}$	$T_{HRSG,out}[K]$
50%	HSR	532,2	485
	LSR	532,2	508,6
40%	HSR	532,2	473,2
	LSR	532,2	502,7
30%	HSR	532,2	453,.5
	LSR	532,2	492,8
20%	HSR	532,2	414,2
	LSR	532,2	473,2

Table 3: Temperature differences in the HRSG depending steam requirement and configuration.

7.5 Discussion.

An overall analysis of the results obtained for the different configurations will assessed. Configuration II resulted to produce the less NPP for all the organic fluids in most of the steam requirement operating conditions. The peak power production for configuration II was around 860 kW for the reference cases when using R113 at high pressure and with a low steam requirement. Moreover, the temperature difference for the three cases was rather high, specially at low pressures. For some cases a pinch point of around 105-110 K was obtained. This low power output from configuration II can be seen in Figure 29.

Configuration I offers the highest power output for most of the steam requirement cases specially for the hydrofluorocarbons, HFCs, R134a and R152a, even so, for these two working fluid ΔT_{pp} was rather high, reaching values from 80 to 90 K, depending on the pressure of themselves. Configuration I also showed to have the highest net power production. In some cases the NPP from the ORC system reached values close to 2 MW of production for high pressures and LSR. In addition to the high NPP, the pinch point for Pentane and R123, was the value design, 15 K, for most of the pressure and steam requirement conditions.

In configuration III, ORC and HRSG are two independent processes. Stability in terms of NPP for configuration III is due to their indecency in respect to the steam generation. Configuration III will only depend then on the load of the engine, thus, the control of the system will be much simpler as only will depend on one variable, instead of depending on the engine load and the steam requirement. On the other hand, the NPP of the ORC system under configuration III is slightly lower for some cases as Figure 29 shows. However, for the three fluids studied in Configuration III, the pinch point remained under acceptable values for R123 and Pentane whereas for R113, ΔT_{pp}, was always the design value. Figure 30 shows the pinch point variation of the system for configuration III.

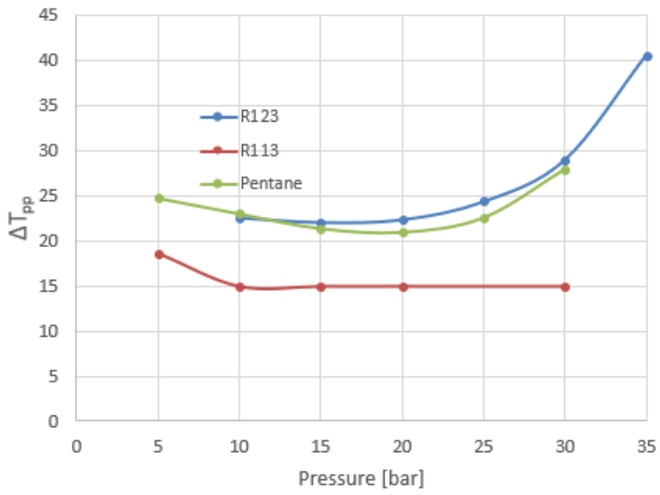

Figure 30: Pinch point variation for Configuration III

To conclude, a Q-T diagram of the ORC boiler using R123 at 30 bar will be displayed in Figure 31 and Figure 32 for Configuration I and Configuration III. For the third configuration, the case where 80 % of the exhaust massflow will be used for the Figure 32. R123 was chosen because their high power output as well as its pinch point remained inside reasonable values. Moreover, R123 is has relatively low values of ODP and GWP and does not propagate flame in a open environment [23].

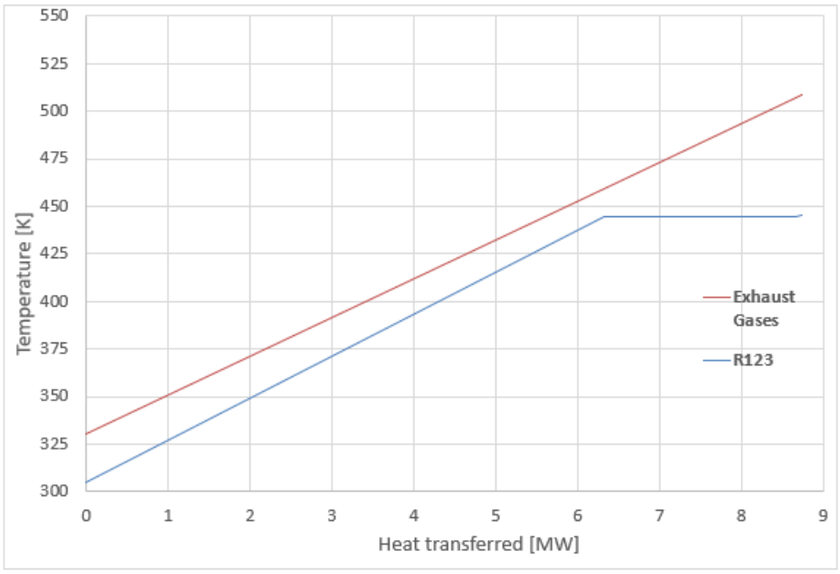

Figure 31: Q-T Diagram for Configuration I using R123 as a working fluid.

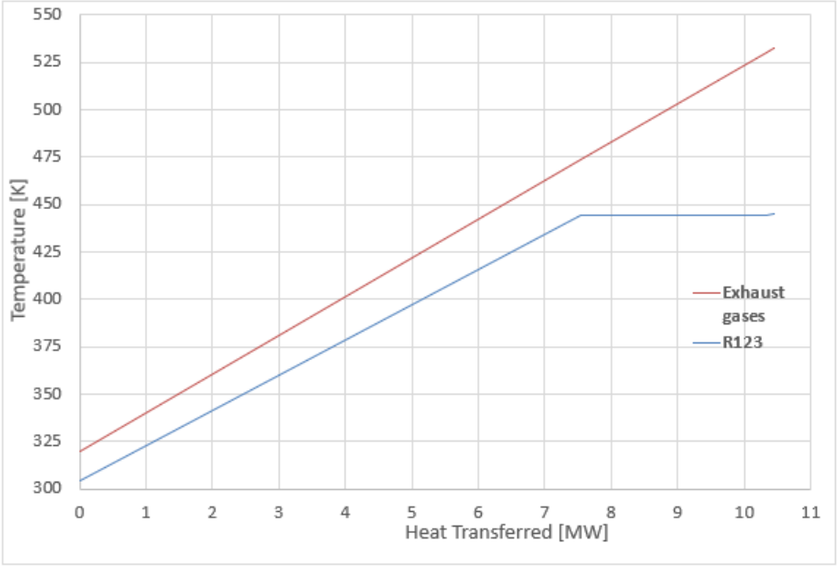

Figure 32: Q-T Diagram for Configuration III using R123 as a working fluid.

As can be seen the pinch point for the III configuration is slightly higher, around 29 K according to Table 19 from Annex I. This is because of the comparison between ORC massflow that the EES model does. For configuration III, the lower ORC massflow was when the pinch point was set at the inlet of the ORC boiler.

8 Conclusion

In this bachelor thesis, a brief review of the organic Rankine cycle components and the behaviour of the ORC installed in a vessel for three different configurations was carried out using exhaust gases as a heat source. The influence of having a HRSG in the system was studied as well. Pinch point and NPP were the main parameters studied in the simulations. Also, the thermal efficiency of the system was calculated as well for all the simulations. In the project, five different organic fluids were used. R134a, R152a, R113, R123 and Pentane were considered to their study although R134a and R152a were not considered to use in configuration II and III as they resulted with rather high values of pinch point. The difference between configurations was the positioning of the HRSG in respect to the ORC system. For configuration I, the exhaust gases flow through the HRSG and the remaining heat is used in the ORC. In the second configuration, the order was reversed. First the exhaust gases flowed through the ORC boiler and then through the HRSG. Configuration III consisted in splitting the exhaust massflow. 50%, 60%, 70% and 80% of the massflow was selected to carry out the project.

The working fluid selection was based on the critical temperature as well as the latent heat of the working fluid as fluids with higher critical temperature showed lower pinch points and those whose latent heat was higher became in higher NPP. Some safety measurements would have to be taken in the case of using Pentane as it shows high flammability [23]. R123 is characterized by low ODP and GWP as Table 1 shows and its power output is one of the highest for configuration I and III as well as for most of the cases pinch point is the design value.

The analysis presented that Configuration I was the best in terms of net power production, for R123 and Pentane a power output of 2 MW was obtained for LSR and high pressure. As in configuration I the system is set along with the HRSG, the steam requirement showed to decrease the output power of the ORC system as the steam requirement was increased, therefore part-load control in the system will be more complicated, as it will depend on the on-board steam requirement and the load of the engine. Configuration II will be discarded for further investigation as it showed the lowest power output for all the working fluids and all the reference cases. Configuration III showed complete stability regardless the steam requirement as they are independent from each other. The NPP varied from 1.700 kW to 1000 kW depending on how much massflow was sent to the system. ORC system showed great energy producing for on-board systems that will represent fuel savings. However, new designs in the integration of the ORC system on board as well as the study of using working fluids that reduce the hazard because flammability or reducing their environmental impact shall be studied in the future.

9 Acknowledgements

This bachelor project could not have been possible without the acceptance from Fredrik Haglind, Maria E. Mondejar Montagud and Enrico Baldasso. Special thanks to Enrico Baldasso for his last minute favors and his help when developing the EES model and clarify doubts. My sincere thanks to DTU, that provided me an opportunity to be an exchange student during my last year in BSc in Mechanical Engineering and also gave me access to the software and other research facilities. Without their acceptance it would have not been possible to carry out this project.

Last but not least, I would like to thank my family: my parents and my brother as they have been supporting me during these entire exchange year.

References

[1] World Shipping Council. The liner shipping industry and carbon emissions policy., 2009.

[2] Pierobon L Larsen U Thern M Haglind F. A Mondejar ME, Andreasen JG. A review of the use of organic rankine cycle power systems for maritime applications. *Renewable and Sustainable Energy Reviews*, 91:126–151, 2017.

[3] Guangrong Zou, Aki Kinnunen, Kalevi Tervo, Mia Elg, Kari Tammi, and Panu Kovanen. Modelling ship energy flow with multi-domain simulation. 05 2013.

[4] B Saadatfar, R Fakhrai, and T Fransson. Waste heat recovery organic rankine cycles in sustainable energy conversion: A state-of-the-art review. 1:161–188, 01 2013.

[5] Austin D. Reid. Low temperature power generation using hfe-7000 in a rankine cycle. 2010.

[6] Costante Mario Invernizzi. *The Organic Rankine Cycle*, pages 117–175. Springer London, London, 2013.

[7] Colonna di Paliano, P and EIM Casati and C Trapp and T Mathijssen and J Larjola and TE Turunen-Saaresti and A Uusitalo. Organic rankine cycle power systems: From the concept to current technology, applications, and an outlook to the future. *Journal of Engineering for Gas Turbines and Power*, 137(10):100801–1–100801–19, 2015.

[8] The specific heat of water. *Proceedings of the Royal Society of London A: Mathematical, Physical and Engineering Sciences*, 85(578):302–304, 1911.

[9] Oyeniyi A. Oyewunmi, Antonio M. Pantaleo, and Christos N. Markides. Orc cogeneration systems in waste-heat recovery applications. *Energy Procedia*, 142:1736 – 1742, 2017. Proceedings of the 9th International Conference on Applied Energy.

[10] Sylvain Quoilin, Martijn Van Den Broek, Sébastien Declaye, Pierre Dewallef, and Vincent Lemort. Techno-economic survey of organic rankine cycle (orc) systems. *Renewable and Sustainable Energy Reviews*, 22:168 – 186, 2013.

[11] Vince Gambino, Payam Ashtiani, and B A. Sc. Once through steam generator (otsg). 06 2018.

[12] Europower-Italy. Elettrogorizia combined cycle project – gorizia, 2006. [Online; accessed 05-April-2018].

[13] Hakan Demir S. Ozgür Atayılmaz Ismail Teke, Özden Agra. Sizing, selection, and comparison of heat exchangers considering the lowest saving-investment ratio corresponding to the area at the tag end of the heat exchanger. 2014.

[14] Linde Engineering. Plate-fin heat exchangers (pfhes). [Online; accessed 06-April-2018].

[15] Danfoss Engineering. All-welded plate heat exchangers (saw). [Online; accessed 06-April-2018].

[16] Gowtham Mohan, Sujata Dahal, Uday Kumar, Andrew Martin, and Hamid Kayal. Development of natural gas fired combined cycle plant for tri-generation of power, cooling and clean water using waste heat recovery: Techno-economic analysis. *Energies*, 7(10):6358–6381, 2014.

[17] Alfred Ongiro, V.I. Ugursal, A Al Taweel, and J.D. Walker. Modeling of heat recovery steam generator performance. 17:427–446, 05 1997.

[18] Roberto Pili, Alessandro Romagnoli, Hartmut Spliethoff, and Christoph Wieland. Economic feasibility of organic rankine cycles (orc) in different transportation sectors. *Energy Procedia*, 105:1401 – 1407, 2017. 8th International Conference on Applied Energy, ICAE2016, 8-11 October 2016, Beijing, China.

[19] Jiansheng Wang, Mengzhen Diao, and Kaihong Yue. Optimization on pinch point temperature difference of orc system based on ahp-entropy method. *Energy*, 141:97 – 107, 2017.

[20] Muhammad Imran, Muhammad Usman, Byung Sik Park, and Dong-Hyun Lee. Volumetric expanders for low grade heat and waste heat recovery applications. 57:1090–1109, 05 2016.

[21] Pardeep Garg, G.M. Karthik, Prashant Kumar, and Pramod Kumar. Development of a generic tool to design scroll expanders for orc applications. *Applied Thermal Engineering*, 109:878 – 888, 2016. Special Issue: Solar Energy Research Institute for India and the United States (SERIIUS) – Concentrated Solar Power.

[22] Pedro J. Mago, Louay M. Chamra, Kalyan Srinivasan, and Chandramohan Somayaji. An examination of regenerative organic rankine cycles using dry fluids. *Applied Thermal Engineering*, 28(8):998 – 1007, 2008.

[23] S Douvartzides and I Karmalis. Working fluid selection for the organic rankine cycle (orc) exhaust heat recovery of an internal combustion engine power plant. *IOP Conference Series: Materials Science and Engineering*, 161(1), 2016.